# Phage Display in Molecular Imaging and Diagnosis of Cancer

Susan L. Deutscher*

*Biochemistry Department, 117 Schweitzer Hall, University of Missouri, Columbia, Missouri 65211, and Harry S Truman Medical Veterans Hospital, Columbia, Missouri 65201*

## Contents

## 1. Introduction

New peptide-based probes to facilitate the molecular imaging of disease are rapidly evolving due to implementation of combinatorial chemistry and bacteriophage (phage) display. Phage display is a powerful technique that allows vast sequence space screening, providing a means to improve peptide affinity and generate unique peptides that bind any given target. Since its inception in 1985, many thousands of peptides have been isolated and investigated using phage display. Such peptides are being explored in vaccine development, enzyme inhibition, inflammation, plant pathology, cardiovascular disease, cancer, etc. The purpose of this review is to analyze and describe those peptides obtained from phage display that have been used successfully in the past five years in both radio and optical in vivo tumor imaging. New tumor targeting agents are required to advance cancer diagnosis and treatment, and phage display selected peptides may be an attractive means to obtain such agents. Unfortunately, the vast majority of the hundreds of peptides

* Tel: 573-882-2454. Fax: 573-882-5635. E-mail: deutschers@missouri.edu.

Susan Deutscher graduated with a Bachelor of Science in Biology from Purdue University in 1980. She received her Ph.D. in Biochemistry at St. Louis University in the laboratory of Dr. Carlos Hirschberg in 1985 where she worked on carbohydrate–protein interactions. After this, she pursued postdoctoral studies at Duke University in the Department of Microbiology and Immunology. She became a faculty member in the Department of Biochemistry at the University of Missouri in 1991 and is currently a Professor there and a Research Chemist at the Harry S. Truman Veterans Hospital in Columbia, Missouri. Her laboratory is interested in the role of carbohydrate and protein–protein interactions in cancer. Work focuses on applying novel combinatorial bacteriophage display approaches and structural biochemistry to characterize these interactions.

selected against tumor antigens have not been shown to function as cancer molecular imaging agents in vivo. Recently, progress has been made in translation of the peptides from in vitro to in vivo applications. Not only have the peptides displayed on phage been employed in vivo as tumor imaging agents, but the phage themselves have been used in imaging with a number of labeling platforms. The integration of phage as not only vehicles for peptide discovery but also as a nanomaterial has wide-ranging applications. Phage display technology is emerging as a powerful, economical, rapid, and efficacious approach to develop new agents for the molecular imaging and diagnosis of cancer.

## 2. Peptides as Molecular Imaging Probes

Molecular imaging probes have aided in our understanding of fundamental biological processes, disease pathologies, and pharmaceutical development.[1–3] Molecular imaging agents that would allow real-time visualization of biomolecules and interactions involved in disease that could also facilitate diagnosis or response to therapy are of particular interest. The targeted molecular imaging of disease processes, particularly tumor growth and metastasis, has been a focus of many investigations for over the last 10 years.[4–9] Enormous progress has been made in both imaging probe discovery
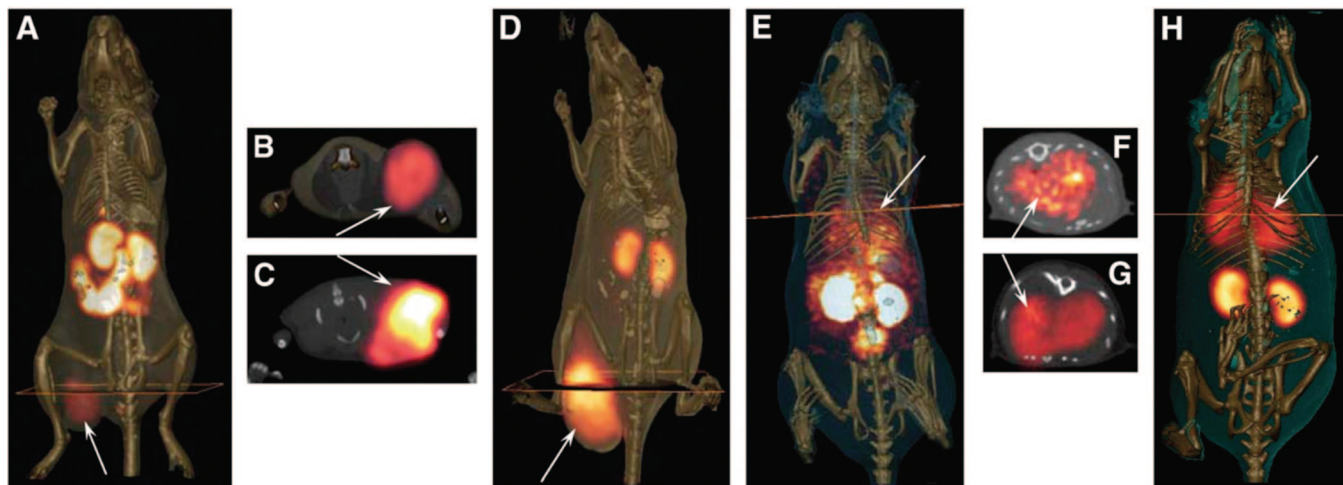
**Figure 1.** SPECT imaging of melanocortin-1 receptor binding α-MSH peptide, CCMSH, in melanoma-bearing mice. Whole-body and transaxial images of $^{99m}$Tc-(Arg$^{11}$)CCMSH (A and B, respectively) and $^{111}$In-DOTA-Re(Arg$^{11}$)CCMSH (D and C, respectively) in B16/F1 flank melanoma-bearing C57 mice at 2 h after injection. Whole-body and transaxial images of $^{99m}$Tc-(Arg$^{11}$)CCMSH (E and F, respectively) and $^{111}$In-DOTA-Re(Arg$^{11}$)CCMSH (H and G, respectively) in B16/F10 pulmonary metastatic melanoma-bearing C57 mice 2 h after injection. Reprinted with permission from ref 24. Copyright 2007 Society of Nuclear Medicine.

and in vivo detection of cancer. In fact, antibodies, nanoparticles, and peptides are being developed for the specific detection of primary and disseminated disease. Undoubtedly antibodies and their fragments are the most common biological targeting vehicles for the specific delivery of an imaging modality to disease sites. Radionuclides, fluorophores, and biotin/streptavidin labeled antibodies have been used successfully to image cancers including those of the breast, prostate, ovary, and others. Radiolabeled antibodies have been employed in cancer imaging and therapy for over 30 years.[10] A classic example is Oncoscint, an $^{111}$In-labeled monoclonal antibody specific for the tumor-associated glycoprotein 72 (TAG-72), which has been used to detect colorectal metastasis lesions.[11] Another example is $^{111}$In-diethylenetriaminepentaacetic acid (DTPA)-trastuzumab, an ErbB-2-targeting antibody that has been used for imaging metastatic breast cancer.[12] Unfortunately, many patients experienced hematological adverse effects and resistance problems after antibody administration with this antibody.[13] Antibodies also exhibit long biodistribution times and slow tumor penetration and clearance rates through the hepatobiliary system.[14] Antibody pretargeting strategies have been developed to evade long circulation times, and antibody fragments have been produced to improve clearance characteristics.[15]

Peptides may offer fundamental advantages over antibodies for in vivo molecular imaging and diagnosis because of their rapid blood clearance, tissue penetration, increased diffusion, nonimmunogenic nature, and straightforward synthesis.[16,17] Their small size may reduce or eliminate side effects that often occur with antibody or antibody fragment-based imaging or therapy applications. However, peptide constructs tagged with a radionuclide or fluorophore may only serve as viable molecular imaging agents if they retain sufficient target affinity. A limited set of regulatory peptides that bind receptors overexpressed on tumors exhibit high affinity (subnanomolar) and are being pursued in imaging and therapy studies. The classic example is octreotide, an eight amino acid cyclized peptide that binds the somatostatin receptor. $^{111}$In-DTPA-octreotide (OctreoScan) has been used successfully to image somatostatin receptor positive tumors in humans.[18] Other natural peptides being explored include

gastrin releasing peptide (GRP) for use in the detection and treatment of prostate, breast, and pancreatic cancer[19] and α-melanocyte stimulating hormone (α-MSH) derivatives for the detection and therapy of malignant melanoma.[20] The CCMSH peptide was cyclized by $^{188}$Re or $^{99m}$Tc for melanoma single-photon emission tomography (SPECT) imaging and therapy (Figure 1).[21–24] 1,4,7,10-Tetraazacyclododecane-1,4,7,10-tetraacetic acid (DOTA) was conjugated to the CCMSH peptide for radiolabeling, while the CCMSH was cyclized by nonradioactive Re. The peptide was labeled with α-particle emitting $^{212}$Pb/$^{212}$Bi for melanoma therapy studies[25] and also with $\beta^+$-emitting radionuclides for positron emission tomography (PET) imaging.[26,27]

## 3. Isolating Phage Display-Derived Peptides

Development of cancer diagnostic and imaging (or therapeutic) compounds has customarily relied on (1) isolation from natural product extracts, (2) screening synthetic compound databases, (3) structure-based rational design, or (4) antibody engineering.[28] An alternative resource for peptide-based imaging agents is through the screening of bacteriophage (phage) display libraries. Phage display was developed by George P. Smith at the University of Missouri in 1985 and was initiated by the finding that *Escherichia coli* (*E. coli*) filamentous phage could be engineered to display foreign amino acid sequences on the tips of certain phage coat proteins (cp) without compromising phage infectivity or propagation ability.[29] Filamentous phage self-assemble into ~900 nm × 6 nm rod-like protein-encapsulated structures, within which is the genetic information to dictate its own production. The genetic encoding of a library allows resynthesis and screening of molecules with a desired binding activity. Amplification of interacting molecules in subsequent rounds of affinity selection can yield peptides that bind to almost any given target. The expression of foreign sequences on phage is not restricted to small peptides; antibody fragments, receptors, and enzymes have been displayed.[30,31] Typically however, in a phage display library, foreign small peptides (5–45 amino acids) are incorporated into the N-terminus of minor coat protein III (cpIII) of fd phage so that at most five copies of the peptide are displayed.[29] Foreign
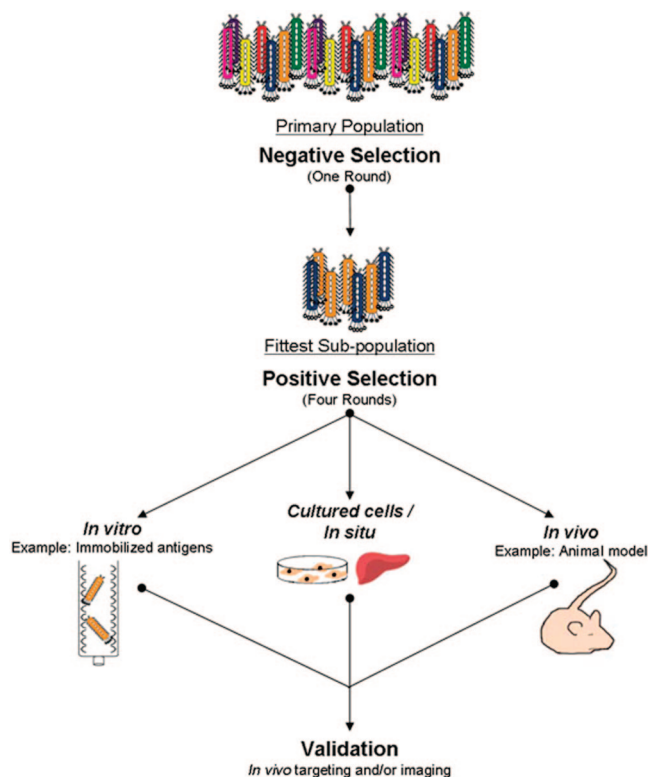
**Figure 2.** Affinity selection using phage display libraries. A phage display library is typically selected against unwanted nonspecific binders before four or five rounds of positive selection. Positive selection can be performed against an immobilized target antigen or tissue culture cells in vitro, in situ, or in vivo. After the last round of selection, validation of phage binding of the desired target is performed in vitro or in vivo.

peptides have also been fused to the major coat protein VIII (cpVIII) of phage so that hundreds or thousands of copies of the peptide can be displayed.[32] Each phage clone displays a single peptide, but a library as a whole may represent $10^9$ peptides, collectively. Peptide libraries are displayed as linear or constrained sequences. Constrained libraries possess two cysteine residues flanking a random segment of peptide, thus facilitating disulfide bond formation. Lytic phage libraries including T7 phage[33] and bacterial display libraries[34] have also been generated. Surface exposure of the foreign peptide on the phage is key to successful screening in that it allows vast numbers of peptides to be easily surveyed for clones whose displayed peptides bind specifically to any given molecular target. Screening of a phage display library typically involves passing the library over the desired target molecules either in vitro, with cultured cells, in situ, or in vivo, capturing bound clones, and washing away unbound phage (Figure 2). Bound phage are often recovered by acid or competitive elution. Captured phage retain infectivity and can be propagated and cloned by infecting fresh host bacteria. The primary structure of the foreign peptide can be elucidated easily by sequencing the peptide-coding sequence in the viral DNA. The affinity selection process is iterative, normally a minimum of four rounds of selection are required to obtain phage enriched for binding.

However, the success of a phage library affinity selection is critically dependent on the stringency employed in all rounds of screening. Affinity selection methods have been adapted in recent years to increase one's chances of obtaining a peptide that binds with good affinity to the desired target. For example, it is quite common to complete an affinity

selection screen of a phage display library, only to find that predominantly selected clones have a much better affinity for the target support (i.e., plastic) than the target. Thus, stringent washing and phage elution conditions are critical. Further, nonrelevant phage can be propagated throughout the selection scheme if they possess superior growth advantages over rare phage that bind the desired target. One means to improve elution of specific phage from the target is to competitively elute with excess free target or ligand. In cultured cell, in situ, and in vivo selections, the target is not known, so nonspecific elution procedures are utilized (Figure 2). These nonspecific elutions consist of extreme pH, high ionic strength, reducing agents, and detergents. Recent reports suggest that these common nonspecific elution methods may not always be strong enough to disrupt phage–target interactions. Thus, the best binding phage may be lost in the affinity selection procedure. Ultrasound has shown improved elution of phage from the target in vitro.[35] Another means to improve the success of affinity selection is to better control the washing conditions throughout the experiment. For in vitro selections, more stringent and controlled washing conditions including selection and washing on macroporous gels or chromato-panning[36] have been proposed. Soh and co-workers have recently developed a microfluidic device involving fabricated ferromagnetic structures to allow for trapping and release of magnetic beads, which facilitates controlled washing using high fluidic forces.[37]

## 4. Phage Display-Derived Tumor-Targeting Peptides

### 4.1. Overview of Selected Peptides

Since its inception almost 30 years ago, phage display has been utilized in vitro, in situ, and in vivo (Figure 2), and thousands of published papers have reported on the isolation of peptides that bind a myriad of targets.[38−57] Phage display libraries have been used most productively to obtain peptide mimics cross-reactive with antibody molecules that could be used for vaccine development. Examples include peptides that bind the antimucin antibody C595,[58] the prostate-specific membrane antigen antibody 4G5,[59] and the ErbB-2 antibody trastuzumab.[60,61] Limited phase I clinical trials are analyzing the T-cell response of many of these peptide-based antibody mimetics.

Far fewer studies have been published on the isolation of phage display peptides that target cancer-associated antigens. Of the roughly 2000 published phage display papers describing peptides to a given target, approximately 8% of these bind to tumors or tumor vasculature (Table 1). The paucity of tumor-targeting peptides in general, is likely a reflection of the complicated events involved in tumorigenesis and a lack of well-defined tumor markers. Nevertheless, peptides have been isolated using in vitro phage display that target several tumor-associated antigens encompassing receptors, vasculature components, lipids, and carbohydrates (Table 1).

### 4.2. In Vitro Selected Peptides

To date, the majority of in vitro selected peptides have not been demonstrated to image tumors in vivo. Peptides that bind in vitro to the proteins CRIP-1 (cysteine-rich intestinal protein),[62] ephrin receptor,[63,64] heat shock protein 90,[65,66] MDM2/p53,[67] interleukin-11 receptor,[68] and prostate specific antigen (PSA)[69] have been reported. Numerous

**Table 1. Tumor Targeting Peptides from Phage Display**

| target | sequence[a] |
|---|---|
| In Vitro | |
| | *Protein/Receptor Target* |
| CRIP-1 (Cys-rich intestinal protein) | CLKDNHRSC[62] |
| ErbB-2 | MARSGL, MARAKE, MSRTMS; **KCCYSL**; WRR, WKR, WVR, WVK, WIK, WTR, WVL, WLL, WRT, WRG, WVS, WVA; MYWGDSHWLQYWYE[55,146,170−172] |
| ephrin receptor (EphA2, EphA4 and EphB) | MQLPLAT, EWLS, SNEW, TNYL, *CVSNPRWKC, CHVLWSTRC*[63,64,115] |
| glucose-regulated protein 78 | WIFPWIQL, WDLAWMFRLPVG; CTVALPGGYVRVC,[65,173] |
| hepsin (prostate cancer) | **IPLVVPLGGSCK**[54] |
| HSP90 | CVPELGHEC[66] |
| interleukin-11 receptor α | CGRRAGGSC[68] |
| melanin | <u>NPNWGPR</u>[147] |
| plectin-1 (pancreatic ductal adenocarcinoma) | **KTLLPTP**[53] |
| PSA (prostate specific antigen) | CVAYCIEHHCWTC,CVFAHNYDYLVC, CVFTSNYAFC[69] |
| MDM2-MDMX/p53 | TSFAEYWNLLSP[67] |
| SPARC | **SPPTGIN**[167] |
| TAG-72 | *VHHSCTKLTHCCQNWH, GGVSCMQTSPVCENNL, NPGTCKDKWIECLLNG,*[174 175] |
| | *Angiogenesis/Lymphatic* |
| FGF receptor | VYMSPF; MQLPLAT[73,74] |
| HUVEC (human colon CA) | CPHSKPCLC[70] |
| HUVEC (gastric cancer) | **CGNSNPKSC**[140] |
| integrin α$_v$β$_3$/α$_5$β$_1$ | **CDCRGDCFC**, CRGDGWC, **XRGDX**, *CQQSNRGDRKRC*[57,104−112] |
| integrin α$_v$β$_6$ | *SPRGDLAVLGHKY*[176] |
| integrin α$_4$β$_1$ | CPLDIDFYC[71] |
| IGF-1 | SEVGCRAGPLQWLCEKYFG[48] |
| lymphatic (leukemia cells) | CAYHRLRRC[103] |
| lymphatic (breast) | <u>CGNKRTRGC</u>[177] |
| lymphatic (rhabdomyosarcoma) | **CMGNKRSAKRPC**[57] |
| MMP-2/MMP-9 | PXX↓(Ser/Thr); CTTHWGFTLC; **SGKGPRQITAL**[141,142178] |
| MMP-11 | A(A/Q)(N/A)↓(L/Y)(T/V/M/R)(R/K)[179] |
| TGF-β receptor | CGLLPVGRPDRNVWRWLC, CKGQCDRFKGLPEWC[76] |
| uPA | **SGRSA**; WGFP; LWXXAr(Ar = Y, W, F, H), XFXXYLW[143,144,180,181] |
| uPAR | AEPMPHSLNFSQYLWYT, **FSRYLWS**,[145,182] |
| VCAM-1 | **VHSPNKK**[50] |
| VEGF receptor | ATWLPPR; HTMYYHHYQHHL[72,75] |
| | *Proapoptotic* |
| protein kinase CK2 | <u>CWMSPRHLGTC</u>[160] |
| phosphatidyl serine | SVSVGMKPSPRP, **CLSYYPSYC**[56,183] |
| | *Carbohydrate/Lectin* |
| TFA | WAY(W/F)SP[49,78] |
| E-selectin | IELLQAR; **DITWDQLWDLMK**[51,52,184] |
| galectin-3 | AYTKCSRQWRTCMTTH, PQNSKIPGPTFLDPH, SMEPALPDWWWKMFK, **ANTPCGPYTHDCPVKR**[148,149] |
| sulfated Lewis A | FAAPMRTVQKID[77] |
| | *Cultured Cell Surface Targets* |
| B-cell lymphoma | CTLPHLKMC, RMWPSSTVNLSAGRR, SAKTAVSQRVWLPSHRGGEP, KSREHVNNSACPSKRITAAL[83−85] |
| cervical carcinoma | C(R/Q)L/RT(G/N)XXG(A/V)GC[87] |
| colon cancer cells | *VHLGYAT*, SPTKSNS, **CPIEDRPMC**, HEWSYLAPYPWF[4,82,88,89,185] |
| glioblastoma | VTWTPQAWFQWV[91] |
| glioma | MCPKHPLGC[186] |
| hepatocarcinoma | TACHQHVRMVRP[92] |
| HUVEC/gastric cancer | CTKNSYLMC[90] |
| NCI-60 binding peptides | EGFR, RVS, AGS, AGL, GVR, GGR, GGL, GSV, GVS[102] |
| neuroblastoma, breast | **VPWMEPAYQRFL**[86,95] |
| non-small-cell lung | *EHMALTYPFRPP*, <u>TDSILRSYDWTY</u>[93] |
| prostate carcinoma | DPRATPGS, FRPNRAQDYNTN[96,97] |
| thyroid cancer cells | *EDYELMDLLAYL*[98] |
| In Vivo | |
| | *In Vivo Selected* |
| prostate carcinoma | GTRQGHTMRLGVSDG, **IAGLATPGWSHWLAL**, YRCTLNSPFFWEDMTHECHA,[119,187] |
| tramp prostate | SMSIARL[101] |
| thyroid carcinoma | HTFEPGV[188] |
| rat tracheal tumor | NRSLKRISNKRIRRK, LRIKRKRRKRKKTRK[189] |
| organ-specific motifs | bone marrow, GGG, GFS, LWS; fat, EGG, LLV, LSP; muscle, LVS; prostate, AGG; skin, GRR, GGH, GTV[100] |

[a] Bold indicates sequences successfully used in imaging. Italic indicates sequences tested via biodistribution studies. Underline indicates sequences utilized in tumor reduction studies.

vasculature and lymphatic binding peptides and peptide motifs have also been identified including those that bind human vasculature endothelium,[70] integrins,[57,71] and growth factor receptors such as fibroblast growth factor (FGF), vascular endothelial growth factor (VEGF), insulin-like growth factor-1 (IGF-1), and transforming growth factor-β (TGF-β).[48,72−76] Peptides that bind the carbohydrate antigens

sulfated Lewis A[77] and Thomsen−Friedenreich (TF),[49] both aberrantly expressed in a variety of adenocarcinomas, have been isolated and well-characterized. Nevertheless, the majority of the aforementioned peptides, while behaving well in in vitro assays, have not been reported to function in vivo.

P30, with the sequence HGRFILPWWYAFSPS, selected against TF antigen is a peptide that does not work well in
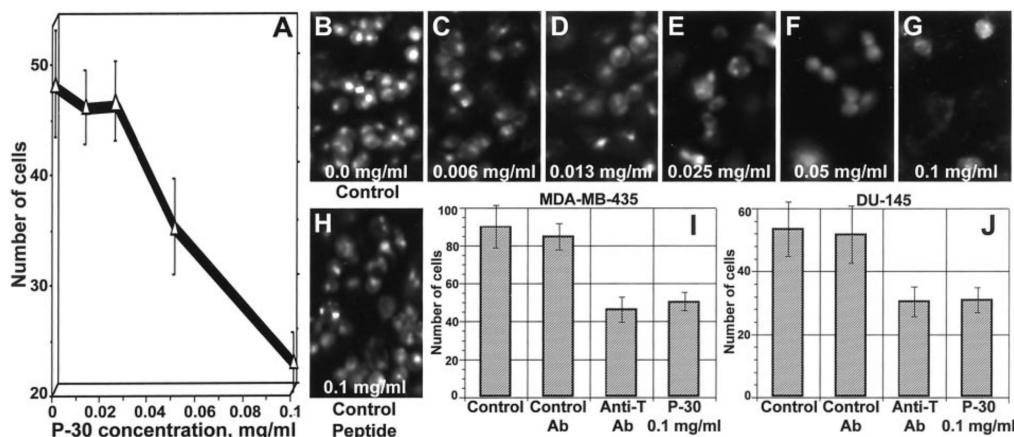
**Figure 3.** Dose-dependent inhibition of 1,1′-dioctadecyl-3,3,3′,3′-tetramethylindocarbocyanine (DiI)-labeled (A) and acridine orange-labeled (B−G) DU-145 human prostate carcinoma cell adhesion to the endothelium by synthetic TF antigen-specific P30 peptide but not by control peptide (H). In panels B−H, numbers at the bottom indicate the concentration of the peptide tested. (I, J) Maximal inhibitory effect on adhesion of MDA-MB-435 human breast carcinoma (I) and DU-145 human prostate carcinoma (J) cells to the endothelium achievable with anti-TF antigen monoclonal antibody and P-30 peptide; bars, SD. Reprinted with permission from ref 5. Copyright 2001 American Association for Cancer Research, Inc.

vivo.[49,78] TF antigen is a Gal$\beta$1−3GalNAc disaccharide expressed on the surfaces of most adenocarcinomas including those of the breast and prostate. TF is involved in adhesion of cancer cells to the endothelium, and the peptide P30 has been shown to inhibit adhesion of MDA-MB-435 breast and DU-145 prostate human cancer cells to human umbilical vein endothelial cells (Figure 3). Furthermore, TF functions to dock cancer cells to the endothelium by interacting with endothelium-expressed galectin-3, which binds TF.[5,6,79] However, the TF-binding peptide P30 has not been shown to bind to or image tumors in vivo.

Combinatorial affinity maturation experiments have been performed on a small number of these peptides, including P30, in an attempt to improve affinity and in vivo binding. Affinity maturation is an in vitro process that purportedly mimics in vivo recombination and selection used by the immune system to compensate for sparse representation in the initial library of sequences related to the optimum sequence. Such affinity maturation studies were performed with the TF-targeting peptide P30 consensus sequence WYAW/FSP in which a 15 amino acid phage library was constructed with random flanking amino acids and reselected against TF. Many of the second-generation peptides had 10-fold improved TF affinity (∼30 nM) and increased binding to TF-positive carcinoma cells but did not bind TF-expressing tumors in vivo.[80,81]

### 4.3. Cultured Cell/In Situ Selected Peptides

Phage display has also been performed using cultured human carcinoma cells or in situ with laser captured microdissected cancer cells[82] resulting in many new peptides as potential imaging probes (Figure 2). Peptides have been selected against cultured human B-cell lymphoma,[83−85] breast,[86] cervical,[87] colon,[4,88,89] gastric,[90] glioblastoma,[91] hepatic,[92] lung,[93,94] neuroblastoma,[95] prostate,[54,96,97] and thyroid[98] carcinoma cells. While the peptides bind the cultured cell lines used in selection, their ability to bind the corresponding xenografted tumors in vivo has not markedly improved over those peptides selected against a purified antigen (Table 1). As shown in Table 1, approximately 20% of the published peptides that reportedly target tumor antigens, vasculature, or lymphatics have been shown to bind to, image, or reduce tumor growth in vivo. In fact, prior to 2007, the success rate of peptides to function in vivo was much less. The meager performance of phage display selected peptides in vivo may be due to the method of selection, the hydrophobic nature of most peptides displayed on phage, poor affinity, or inability of the peptides to function outside the phage framework.

### 4.4. In Vivo Selected Peptides

It has been argued that in vivo phage display selection procedures theoretically offer an advantage over in vitro or in situ screening procedures in that phage can be selected in the complicated milieu of the animal based on desired pharmacokinetic properties including delivery and tumor accumulation. Such a selection does not rely on knowledge of the target. Further, the selected peptides can allow identification of the target antigen using database search analyses and biochemical approaches such as affinity chromatography and mass spectrometry. More than 10 years ago Pasqualini and Ruoslahti performed phage peptide library selections in vivo and isolated peptides with motifs that targeted the vasculature of various organs and tumors, most notably RGD and NGR motifs.[99−102] Tissue-specific peptides have been identified that bind brain, breast, lung, fat, pancreas, skin, etc.[100,103] A variety of RGD-containing peptides that bind $\alpha_v\beta_3$ integrin have been described by numerous groups.[57,104−112] Vascular endothelial lymphatic-targeting motifs have also been described using in vivo phage display.[57,113] Tumor vasculature receptors targeted by some of these peptides have been identified including interleukin 11 receptor,[100] aminopeptidase P,[114] and the EphA4 receptor.[115] However, in vivo phage display has predominately identified peptides that bind to tumor vasculature components and not directly to tumor cells (Table 1). Nevertheless, many of these peptides are showing great promise not only in vitro but also in targeting in vivo in a variety of disease models.[116]

Discovery of tumor-cell surface targeting agents in addition to tumor vasculature targeting agents is also being pursued. Procedures have recently been devised to obtain phage that extravasate the vasculature and home to tumor cell-associated antigens in vivo.[117−119] Key steps to the in vivo selection of tumor-targeting phage included preclearing of libraries of vasculature-targeting phage in vivo by isolating phage in the circulation, appropriate biodistribution times,[120] detergent extraction of phage from target tissues, and large scale mass

**Table 2. In Vivo Phage Display Selected Peptides against PC-3 Prostate Tumors**[a]

| f88-Cys6 library selection in PC-3M tumor bearing SCID mice | | f88-Cys6 library selection in PC-3 tumor bearing SCID mice | |
| --- | --- | --- | --- |
| phage clone | sequence | phage clone | sequence |
| A1 | TDVSCKNHKGACCSTN | E1 | INTECAGLGLVCKPHT |
| A2 | HIEPCVPGWVGCNSLI | E2 | NKSKCRCRQNACKQLI |
| A3 | EKFFCNTVNRGCTGPQ | E3 | CTSSCKPHSQSCKEKT |
| A4 | HMQQCKKRTTRCKVQS | E4 | NKKQCKTVLKMCHRRV |
| A7 | IKNNCGPVWEVCVQYP | E5 | DRPHCLKTWNICTSYY |
| A8 | KNLTCWNEEYQCGWKV | E6 | MKRECKNRCALCKSER |
| A9 | TMNWCNHNPMTCGSQF | E7 | IVPGCSKTERGCSYQS |
| A12 | PTIMCKKQEKLCRLRM | E10 | KPSPCSSFKSHCVRRD |
| B3 | PTKRCVRQDEICNNKR | E11 | AKYYCEELVNHCTSAQ |
| B4 | PQEMCTCMARGCRWKT | F1 | GDLRCRITKQKCEQQC |
| B9 | DETPCQHYGNCCTLIL | F8 | ETIMCIRYRCDCPLPH |
| B10 | YKCLCAAGASTCQPGP | *F11* | *GPAHCKRTISQCQTNE* |
| B12 | VQRSCIQAPKECYTDK | G2 | DEWHCKFNGAVCTSMR |
| C1 | KIDSCEWTAKYCISEI | **G1** | **IAGLATPGWSHWLAL** |
| C2 | PDQLCQPEESECGTLP | G5 | QRVTCDMAENCCPKTS |
| C5 | NVMACSCTHGWCITKT | G10 | PPRLCQGMRGTCSGNQ |
| C8 | ESMQCETSQNKCLTTR | G12 | CACICPCNPAFCTVAV |
| C9 | LKTRCISNSPHCNYSD | H1 | KMPECHEQQEYCDGDR |
| C10 | NKSQCSKWRASCDIPR | H2 | QKEHCILHTANCGRIT |
| C11 | TRNPCKKAKMVCEEWP | H4 | TNTNCGTDLEPCVSTM |
| D2 | DQRACKNSILTCMKAG | H6 | HDKQCLTAKDRCGTIK |
| D6 | LSNCCETPCAYCYLSP | H12 | ASCECNPHPRHCGETR |

[a] Bold indicates sequences successfully used in imaging. Italic indicates sequences tested via biodistribution studies.

propagation and amplification of phage.[119] In one study, prostate tumor-homing peptides were isolated from PC-3 and PC-3 M human prostate tumor xenografts in vivo. In these studies, $1 \times 10^9$ infectious units of a precleared random peptide library fused to either cpIII (f3−15-mer) or cpVIII (f88−15-mer and cysteine constrained f88/cys6) were injected into human prostate tumor-bearing SCID mice for 1 h. Animals were perfused and sacrificed, tumors were removed and washed, phage were eluted in 0.5% CHAPs detergent buffer, and the entire phage population was allowed to infect host *E. coli* for a round of amplification. The selections were repeated four times. Representative sequences of displayed peptides that were selected after the final round from the cys6 library are shown in Table 2. Micropanning experiments of individual phage clones with cultured prostate carcinoma cells and excised prostate tumors indicated that ∼20% of the selected phage bound prostate carcinomas but not normal prostate.[119] The phage clones F11 and G1 bound well to PC-3 human prostate cultured carcinoma cells and xenografted tumors but not to normal cells or tissue. Binding of AlexaFluor (AF) 680-labeled G1 phage to cultured PC-3 prostate carcinoma cells is shown in Figure 4.

In vivo selections often do not result in a predominant phage clone, but rather hundreds of thousands of different phage clones displaying unique sequences that need to be analyzed for binding. This highlights the difficulty in predicting which displayed peptide sequence from an isolated phage clone, once chemically synthesized, will function in vivo. High-throughput, peptide database and search algorithms and mass DNA sequencing approaches[121,122] may facilitate deconvolution of functional and specific phage for corresponding peptide synthesis.

## 5. Labeling Peptides for Molecular Imaging

### 5.1. Radiolabeling Peptides

Peptides have been labeled with radionuclides, fluorophores, and other tags for molecular imaging. Radiolabeled peptides have shown the most success in imaging tumors in
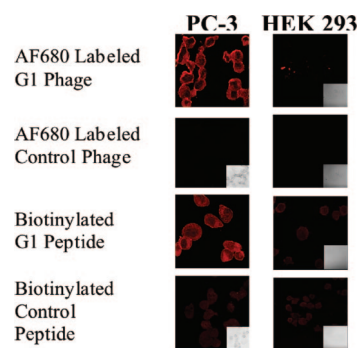


**Figure 4.** Binding of AF680-labeled phage and peptide to PC-3 human carcinoma cells and control HEK 293 cells. Slides containing fixed PC-3 or human embryonic kidney (HEK 293) cells were incubated with AF680-labeled phage ($1 \times 10^{11}$ virion/mL) or biotinylated peptide (20 $\mu$M) at room temperature for 1 h in the dark. Binding of peptides was detected using NeutrAvidin−Texas Red.

animals. The efficacy of radiolabeled peptides as imaging agents is closely associated with the radionuclide and chelate employed. One of the commonly employed radionuclides for use in SPECT imaging is $^{99m}$Tc due to its nuclear properties (6 h half-life, 140 keV gamma emission) and ready availability.[123,124] Most hospitals are equipped with SPECT imaging equipment and personnel trained in image acquisition and interpretation. Development of radiopharmaceuticals based on $^{99m}$Tc has been advanced by the use of "click" $^{99m}$Tc-carbonyl chemistry.[125] Another widely used radioisotope for labeling peptides that can be used in diagnostic SPECT is $^{111}$In, which has a 2.8 day half-life and emits gamma photons with energies of 173 and 247 keV.[18,126]

PET coupled with the $\beta^+$-emitting tracer fluorine-18 2-deoxy-2-fluoro-D-glucose ($^{18}$F-FDG) is commonly used in studying cell metabolism and disease.[127] $^{18}$F-FDG is currently the primary PET tracer utilized for imaging processes with increased glucose metabolism including cancer.[128] PET has some advantages over SPECT in that it is 1−2 orders of magnitude more sensitive and is quantitative.[127] PET tracers are being developed that target specific receptors or antigens

on tumors, since the uptake of ^{18}F-FDG is not increased in all cancer cells. ^{64}Cu-labeled complexes are being explored because the radiometal has favorable properties for PET imaging and therapy due to its half-life ($t_{1/2} = 12.7$ h) and two different decay modes ($\beta^+$ 17.4%, $\beta^-$ 39%).[126,129] Another PET isotope showing recent promise in imaging is gallium-68. [68]Ga is a short-lived positron emitter with high specific activity that can be routinely made from a [68]Ge/^{68}Ga generator[130,131] and appended to peptides. The 68 min short half-life of ^{68}Ga is ideal for the pharmacokinetics of radiopharmaceuticals with low molecular weight such as peptides.

## 5.2. Bioluminescent and Fluorescent Labeling

Noninvasive real-time in vivo imaging of biological processes and diseases including cancer is receiving much attention of late. Traditional methods for imaging including X-ray, magnetic resonance imaging, SPECT, and PET, which, while suited for large masses or whole body imaging, have their limitations for monitoring more microscopic processes in real-time. Because of this, considerable effort has been placed on developing bioluminescent and fluorescent imaging systems. The use of bioluminescence to tag cells, pathogens, genes, and proteins can provide insights into biochemical mechanisms in the living organism.[8,132,133] Advances in instrumentation for detecting weak optical signals coupled with a better appreciation of the optical properties of tissue have allowed for detection and quantification of signal in vivo.[7] In bioluminescent imaging, cells produce bioluminescent proteins such as luciferase and generate light with appropriate substrates.[8] Analyses of the light produced in vivo reveals the spatial and temporal distribution of the biological process under investigation including cell growth, adhesion, apoptosis, metastasis, etc. In fluorescent imaging, an external source of light is required for excitation of the fluorophore. Wide ranges of fluorescent molecules have been expressed in cells.[133] Additionally, nanoparticles and quantum dots (Qdots) have been used for in vivo imaging.[134] The near-infrared fluorophores (NIRFs) with long emission wavelengths theoretically provide optimal optical images in vivo. NIRFs that emit between 700 and 900 nm have shown the most promise because tissue absorption from chromophores and nonspecific autofluorescence are minimal at these wavelengths. Accepted NIRFs used for in vivo imaging in animals include AF680 and Cy5.5 (680 nm absorption, 720 nm emission), IRDye800CW (774 nm absorption, 789 nm emission), and IC-green (780 nm absorption, 820 nm emission).[135,136] Various studies have shown the efficacy of optical imaging probes using these fluorophores for breast cancer diagnosis and imaging of lymphatics.[136,137] However, the fluorescent imaging of deep tissue targets is challenging because it is difficult to accurately deconvolute the light signal produced from deep in tissues due to interference from bodily materials that alter light scattering and emitted light absorption.

Because no single imaging modality is ideal, efforts are also focused on developing multimodal imaging agents that take advantage of the strengths of each imaging technique employed.[138] For instance, Gelovani and co-workers labeled an RGD peptide with the NIRF IRDye800 and ^{111}In for dual optical and SPECT imaging of human melanoma xenografts.[139] While both optical and gamma scintigraphy were able to detect the tumor, the optical images were superior in terms of resolution and detection of superficial tumors, and SPECT images were better at detecting deeper tumors.

## 6. Phage Display-Selected Peptides Used for in Vivo Molecular Imaging of Cancer

## 6.1. Success Stories

While the vast majority of publications on phage display-selected peptides have only reported the use of peptides in vitro, there are a small number of phage display peptides that have been radiolabeled and used in SPECT and PET imaging or tagged with biotin or a fluorophore for use in optical imaging of cancer in vivo. As highlighted in Table 1, various peptides isolated from phage display screens are showing promise as potential targeted in vivo radio and optical imaging probes. Peptides used successfully to image tumor vasculature or lymphatics include $\alpha_v\beta_3$-integrin-binding RGD-containing peptides,[57,104−107,109,111,112] gastric cancer endothelium-binding CGNSNPKSC peptide,[140] vascular cell adhesion molecule-1-targeting (VCAM-1) VHSP-NKK peptide,[50] matrix metalloproteinase (MMP)-2/9-targeting CTTHWGFTLC and SGKGPRQITAL peptides,[141,142] urokinase plasminogen activator (uPA)-binding SGRSA peptide[143] and urokinase-type plasminogen activator receptor (uPAR)-homing FSRYLWS peptide.[144]

In one study, a T7 phage display library was selected against rhabdomyosarcoma cultured cell lines and an RGD-containing $\alpha_v\beta_3$-binding peptide and a lymphatic binding peptide with similarity to LyP-1 were isolated. The Lyp-1-like peptide, CMGNKRSAKRPC, was biotinylated and used in vivo to demonstrate that the peptide localized to neuroblastoma tumor vasculature.[57] In another study, a FSRYLWS variant peptide, which binds to loop three of uPAR domain III, was labeled via DOTA with ^{64}Cu and used to PET image U87MG glioblastoma tumors in rodents. Tumor accumulation was 8.1 %ID/g at 6 h postinjection.[145] uPA and uPAR are key players in MMP degradation of extracellular matrix in the tumor environment and are promising tumor targets for prostate cancer diagnosis and therapy.

Most of the peptides identified from phage display selections that have been used in molecular imaging in vivo bind vasculature components. However, proteins overexpressed on tumors have also been targeted by phage display-selected peptides for in vivo imaging. The ErbB-2-targeting peptide KCCYSL,[55,146] melanin-targeting peptide NPN-WGPR,[147] hepsin/prostate cancer targeting peptide IPLV-VPLGGSCK,[54] plectin-1/pancreatic ductal adenocarcinoa targeting peptide KTLLPTP,[53] and the galectin-3-targeting peptide ANTPCGPYTHDCPVKP,[148,149] have been used monovalently, on phage or nanoparticles, to image tumors in vivo. An example of a linear peptide functioning to image tumors in vivo is the galectin-3-binding peptide ANTPCG-PYTHDCPVKP. Galectin-3 binds terminal galactopyranose residues on carbohydrates, most notably those of TF antigen (Figure 3). TF−galectin-3 association triggers relocalization of galectin-3 to cell surfaces of tumor cell−endothelial cell contact. The ANTPCGPYTHDCPVKP peptide, isolated from a cysteine-constrained library engineered in George Smith's laboratory,[148] inhibited TF−galectin-3 interaction by ~50%. Its ability to localize to tumor endothelium expressing galectin-3 was demonstrated by in vivo biodistribution and SPECT imaging studies with an ^{111}In-DOTA version of the peptide in human MDA-MB-435 breast tumor-bearing mice. In vivo biodistribution studies revealed that tumor uptake was $1.2 \pm 0.24$, $0.75 \pm 0.05$, and $0.6 \pm 0.04$ (mean $\pm$ SD) percent injected dose per gram (%ID/g) at 0.5, 1.0, and 2.0 h postinjection of the radiotracer, respectively. However, high
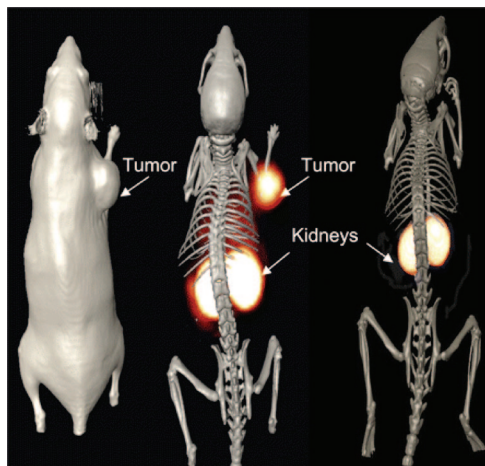
**Figure 5.** Tumor imaging with ^{111}In-DOTA(GSG)-ANTPCG-PYTHDCPVKR peptide. MDA-MB-435 breast tumor-xenografted SCID mice were injected in tail vein with 11.1 MBq of ^{111}In-DOTA(GSG)-ANTPCGPYTHDCPVKR peptide and imaged in a MicroCAT II (Siemens Medical Solutions) dedicated small-animal SPECT/CT scanner equipped with high-resolution 2-mm pinhole collimator. SPECT images were fused with conventional CT images to validate regions of increased radiolabeled ligand uptake. At left is volume-rendered CT image, at center, coregistered SPECT/CT radioligand uptake image of galectin-3-avid peptide, and at right, SPECT/CT image of scrambled peptide. Imaging was performed 2 h after injection. Reprinted with permission from ref 149. Copyright 2008 Society of Nuclear Medicine.

kidney uptake (~22 %ID/g) was observed at 2 h. SPECT/CT studies with ^{111}In-DOTA-glysergly(GSG)-ANTPCG-PYTHDCPVKP showed good tumor uptake and contrast in the tumor-bearing mice (Figure 5). Specificity of peptide binding was demonstrated by successful blocking (52%) of in vivo tumor uptake of ^{111}In-DOTA(GSG)-peptide in the presence of its nonradiolabeled counterpart at 2 h post injection.

One of the best examples of a phage display-selected peptide used successfully in tumor imaging is the ErbB-2-targeting peptide KCCYSL. KCCYSL was obtained from a six amino acid fUSE5-cpIII phage library generated in George P. Smith's laboratory.[29,146] ErbB-2 is a member of the epidermal growth factor receptor (EGFR) family of transmembrane receptor tyrosine kinases. While no known ligand or growth factor has been identified for ErbB-2, it heterodimerizes with other family members activating several signaling pathways resulting in increased cancer cell adhesion, growth, angiogenesis, and cell survival.[150,151] ErbB-2 has received much attention both as a biomarker for breast and prostate cancer and as a target for specific cancer imaging and therapeutic agents. Antibodies such as trastuzumab (Herceptin; Genetech, Inc.) have been developed to target or block the action of ErbB-2 and have been radiolabeled with a myriad of radionuclides for cancer imaging and therapy.[152,153] KCCYSL was shown to bind the extracellular domain (ECD) of ErbB-2 with 295 nM affinity and to bind cultured carcinoma cell lines that express ErbB-2 including breast, prostate, and ovarian cancer cell lines. The ErbB-2-targeting peptide KCCYSL may function as a mimic of a CCY/F motif present in EGF-like domains of ErbB family member ligands.[146] The KCCYSL peptide was conjugated with DOTA via a GSG spacer and radiolabeled with ^{111}In for the SPECT imaging of ErbB-2-positive tumors.[55] The ^{111}In-DOTA-GSG-KCCYSL peptide bound ErbB-2-expressing human MDA-MB-435 breast carcinoma cells in vitro,

and competition studies with nonradiolabeled peptide revealed an $IC_{50}$ value of 42.5 ± 2.76 nmol/L (Figure 6). Biodistribution studies showed rapid tumor uptake and whole body clearance of ^{111}In-DOTA-GSG-KCCYSL in human breast carcinoma-bearing SCID mice, and SPECT/CT studies demonstrated that the breast tumor was readily visualized by the radiolabeled peptide conjugate at 2 h post injection (Figure 7). The only nontarget organ uptake was in the kidneys.

## 6.2. Kidney Uptake of Radiolabeled Peptides

Although radiolabeled peptides are excellent targeting moieties, their short plasma half-life and high renal retention will need to be improved for translation into humans, especially if employed as therapeutic agents. Radiolabeled peptides as well as small antibody fragments are cleared from the kidney, which is the preferred route of elimination of a radiopharmaceutical. High kidney uptake has been observed for most of the commonly studied radiolabeled peptides[154−156] and is also evident with phage display-selected peptides (Figures 5 and 6). For imaging purposes, renal uptake greatly reduces the sensitivity of detection if the tumor is in the vicinity of the kidney. For therapy, renal accumulation of radiolabeled molecules limits the maximum tolerated dose that can be administered without radiation-induced nephrotoxicity. Thus, lowering the renal uptake would allow for administration of higher tumor radiation doses and improved therapeutic response. Numerous approaches have been investigated to alter renal retention of radiopharmaceuticals. Standard approaches of changing peptide sequence and charge, radionuclide, or chelate have shown limited success. Coadministration of basic compounds, particularly lysine or arginine can reduce radioactive uptake in the kidney by on average 50%;[155−157] however high doses of these amino acids can cause serious side effects including arrhythmia, hyperkalemia, and nephrotoxicity.[158] More recently, plasma substitutes that cause low molecular weight proteinuria by decreasing tubular reabsorption have been investigated with similar results as amino acid infusions.[159] Additional means to reduce kidney uptake are thus warranted.

## 6.3. Peptides in Tumor Reduction

Not only have phage display-selected peptides been used in cancer imaging, but they have also been used in vivo to reduce tumor growth. The ability of unlabeled peptides to functionally modulate tumor growth and spread should positively impact future studies aimed at developing peptide-based cancer therapeutics. Potentially harmful radiation-induced damage to nontarget organs will be avoided if unlabeled peptides can be employed. Previous studies have relied on chemotherapeutics or antibodies (which often cause immune response problems). There have been a few reports of the use of phage display-selected peptides in vivo to lessen tumor growth (Table 1). In a 2008 study, a protein kinase (CK2) inhibitor cyclic peptide CIGB-300 blocked CK2 phosphorylation and reduced cervical tumor growth in heterotransplanted nude mice. Further, the safety of CIGB-3000 administration was evaluated in 31 women with cervical cancer. The peptide was well tolerated and reported to reduce cervical lesions in the majority of patients.[160] In 2009, Chang and co-workers reported that a non-small-cell lung cancer (NSCLC)-targeting peptide TDSILRSYDWTY, when coupled to liposomes with doxorubicin or vinorelbine, increased the
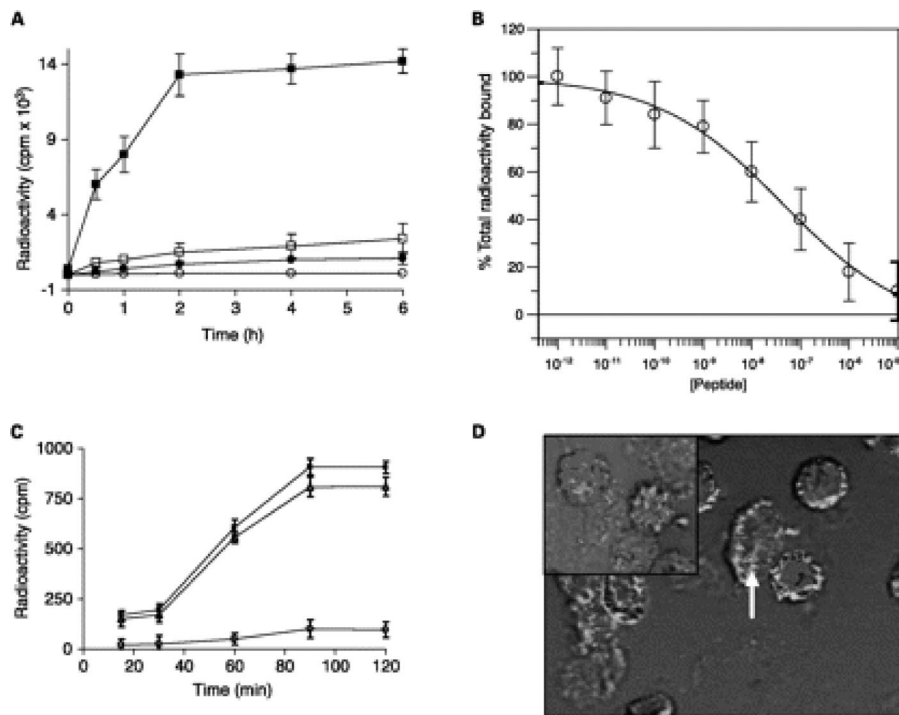
**Figure 6.** The ErbB-2 receptor binding properties of the radiolabeled ^{111}In-DOTA(GSG)-KCCYSL: (A) ~1.0 × 10^6 cells per well were incubated at 37 °C for different time intervals with 5 × 10^4 cpm radioligand. Whereas significant radioligand binding to human MDA-MB-435 breast carcinoma cells was observed (■), minimal binding was observed with K-562 human chronic myeloid leukemia cells (●). Little binding of a radiolabeled scrambled peptide KYLCSC was observed with MDA-MB-435 (□) or K-562 (○) cell lines. Points represent the mean of three replicates; bars represent SD; $P < 0.001$. (B) Displacement of ^{111}In-DOTA(GSG)-KCCYSL peptide by its nonradiolabeled counterpart. MDA-MB-435 cells were incubated with 6 × 10^4 cpm radioligand and increasing concentrations of the nonradioactive peptide. The $IC_{50}$ value obtained was 42.5 ± 2.76 nmol/L. Points represent mean of three replicates; bars indicate SD. (C) Determination of percent internalized radioactivity in human MDA-MB-435 breast carcinoma cells. Cells (3 × 10^5 per tube) were incubated at 37 °C with ^{111}In-DOTA-(GSG) KCCYSL (4 × 10^4 cpm). The total (■), surface-bound (△), and internalized (○) radioactivity (cpm) as a function of time is depicted. Points represent mean of two replicates; bars indicate SD; $P < 0.001$. (D) Surface binding and internalization of 5-carboxyfluorescein (FAM)-(GSG)-KCCYSL peptide. MDA-MB-435 cells were incubated with 0.5 $\mu$mol/L fluorescent peptide for 45 min at 37 °C. After washing, the cells were fixed in paraformaldehyde and analyzed by confocal microscopy with an excitation/emission wavelength of 490/520 nm. The majority of the peptide was surface bound. Arrow indicates potential internalized peptide. Inset shows analysis with FAM(GSG)-KYLCSC peptide indicating no binding. Reprinted with permission from ref 55. Copyright 2007 American Association for Cancer Research, Inc.

efficacy of the chemotherapeutics and survival rates of NSCLC-xenografted mice.[94] Thus, a promising application of phage display peptides may not only be for imaging of molecular processes and diseases but inhibition of steps involved in disease progression.

## 7. Phage as Molecular Imaging Agents

### 7.1. Radiolabeled Phage

Phage displaying tumor-homing peptides have shown recent promise as tumor imaging agents. In fact, there are more reports of peptide-displaying phage used in tumor imaging then the corresponding synthesized peptides (Table 1). There are many attributes of phage that uniquely suit them as in vivo imaging agents and biological nanoparticles. Filamentous phage self-assemble into long (~900 nm × 6 nm) rod-like protein-encapsulated structures, within which is the genetic information to dictate their own production. Phage can be covalently attached to numerous tags such as biotin or fluorophores such as AF680 while simultaneously expressing multiple copies of foreign vasculature or tumor-targeting peptides. This results in signal amplification. Phage have also been physically well-characterized, are resistant to harsh conditions, and are nonpathogenic. Studies have shown that fd phage are well tolerated at high concentrations in vivo and generate only a weak immune response after

weeks of administration.[120] Given this, they may be superior to commonly employed inorganic nanoparticles for in vivo imaging.

A few laboratories have been developing phage into agents for use in SPECT and PET radioimaging.[119,161−163] Initial studies demonstrated that ^{99m}Tc-labeled phage could be used in vivo to image bacterial infections in mice.[161,162] This approach has been extended to tumor imaging in vivo. For tumor imaging, it would seem that the most straightforward approach would be to covalently couple a radiometal bifunctional chelator onto the phage for direct labeling. However, phage radiolabeled with ^{99m}Tc via a mercaptoacetyltriglycine chelate demonstrated high liver uptake of radioactivity (10−40 %ID/g). This finding is consistent with the long clearance time of approximately 72 h of phage through the reticuloendothelial system (RES).[120] Hence, implementation of a pretargeting system with phage may allow for phage clearance before administration of the radiolabel. Both two-step and three-step pretargeting strategies with biotinylated phage have been reported for the SPECT imaging of cancer.[163,164] The in vivo selected prostate tumor-targeting phage clone G1 (Tables 1 and 2; Figure 4) was used in a two-step system with biotinylated phage in combination with ^{111}In-radiolabeled diethylene triamine pentaacetic acid (DTPA)-streptavidin. Results were compared with a three-step pretargeting method utilizing biotinylated
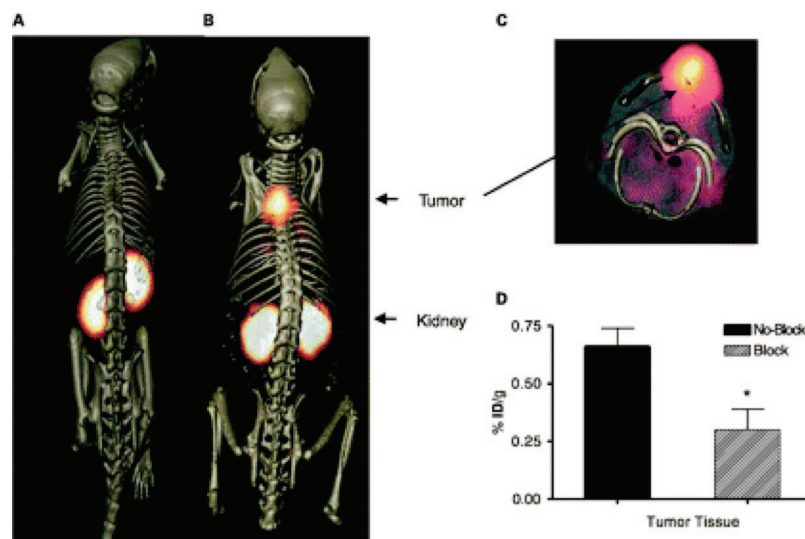
**Figure 7.** Tumor imaging with $^{111}$In-DOTA(GSG)-KCCYSL peptide. MDA-MB-435 breast tumor-xenografted SCID mice were injected in the tail vein with 11.1 MBq of $^{111}$In-DOTA(GSG)-KCCYSL or $^{111}$In-DOTA(GSG)-KYLCSC scrambled peptide and imaged in a microSPECT scanner. The SPECT images were fused with conventional microCT images to validate regions of increased radiolabeled ligand uptake: (A) coregistered microSPECT/CT radioligand uptake image with $^{111}$In-DOTA(GSG)-KYLCSC; (B) coregistered microSPECT/CT image with $^{111}$In-DOTA(GSG)-KCCYSL; (C) microSPECT/CT image axial view focusing on tumor uptake of the radioligand; (D) in vivo blocking studies with $^{111}$In-DOTA(GSG)-KCCYSL in MDA-MB-435 breast tumor-xenografted SCID mice. Fifteen minutes after injection of the nonradiolabeled In-DOTA(GSG)-KCCYSL ($10-5-10-12$ mol/L) peptide, 0.11 MBq of radiolabeled counterpart was injected and the blocking efficiency was evaluated after 2 h. A 50% block of the radiolabeled peptide binding to the tumor tissue was observed. Columns represent mean of three animals for each experiment; bars indicate SD; * indicates $P < 0.001$. Reprinted with permission from ref 55. Copyright 2007 American Association for Cancer Research, Inc.
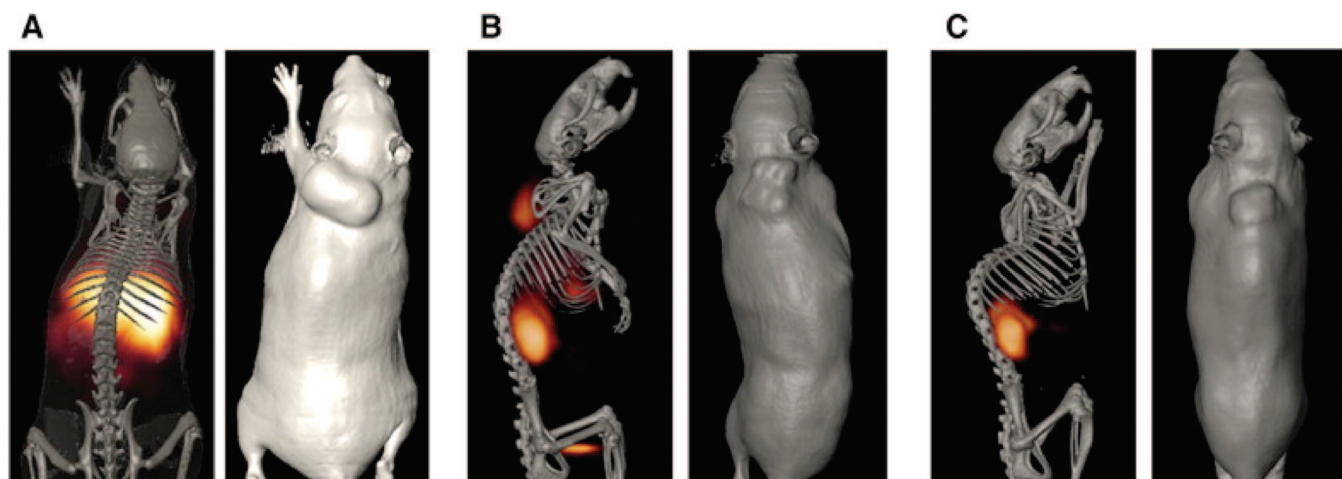


**Figure 8.** SPECT/CT imaging studies of pretargeted $^{111}$In-labeled streptavidin and biotin in SCID mice bearing human prostate PC-3 carcinoma tumors. SCID mice bearing human PC-3 prostate carcinoma tumors received tail vein injections of $10^{11}$ virions of biotinylated G1 phage. (A) Four hours after injection of the biotinylated G1 phage, mouse A received an injection of 7.40 MBq of $^{111}$In-DTPA-SA for the purpose of two-step pretargeting by biotinylated G1 phage. The image was taken 24 h after injection of the radiolabel. (B, C) Mice B and C received three-step pretargeting treatments. Four hours after injection of the biotinylated G1 phage both mice received an injection of avidin, which was allowed to circulate and clear the body for 24 h. Mouse B then received a third injection of 7.40 MBq of $^{111}$In-DOTA-biotin, while the third injection given to mouse C contained both cold In-DOTA-biotin and $^{111}$In-DOTA-biotin. All mice were euthanized before 15 h of scan data were obtained. Reprinted with permission from ref 164. Copyright 2009 Elsevier.

phage, avidin, and $^{111}$In-bisbiotin. Biodistribution studies revealed there was high radioactive uptake in the two-step pretargeting approach in the liver, kidneys, and intestines at 24 h, which may be attributed to the pharmacokinetics of $^{111}$In-streptavidin. However, there was less than 1 %ID/g radioactivity in the tumor. In contrast, there was good (~3 %ID/g) uptake of radiolabel in the tumor using the three-step approach and less kidney uptake (5% ID/g at 1 h). Very little radioactivity accumulated in other organs including the liver. Taken together, these results suggest that a three-step pretargeting approach may yield the best phage-based radioimaging probe. The ability of G1 phage to act as SPECT imaging agents of human PC-3 prostate tumor heterotransplants in mice using both the two-step and three-step methods is shown in Figure 8.[164] As shown, SPECT images of G1 phage using the two-step approach did not show tumoral accumulation, whereas the prostate tumor was clearly imaged using the three-step scheme.

## 7.2. Fluorescent Labeled Phage

A review of the literature suggests that phage display has been most successfully used in molecular imaging by employing fluorescently tagged phage or nanoparticle plat-
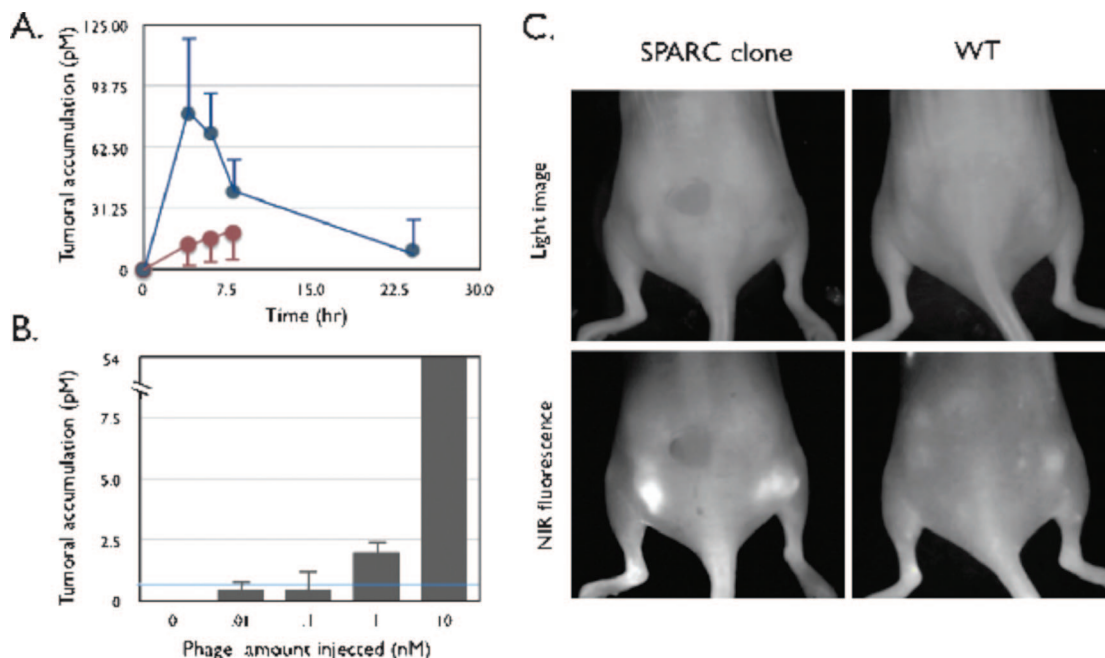
**Figure 9.** In vivo behavior of labeled phage. (A) Time course of tumor homing. Mice bearing subcutaneous bilateral LLC-derived tumors were coinjected through the tail vein with VT680-labeled SPARC-targeted phage and AF750-labeled wild-type phage (no insert) and imaged at 0, 2, 4, 6, and 24 h after injection: (blue) SPARC-targeted phage clone 23; (brown) wild-type phage (no insert). (B) Detection threshold. Tumor-bearing mice were injected with increasing log doses of labeled phage and imaged 4 h after injection. The line indicates detection threshold. (C) Reflectance imaging. Mice bearing subcutaneous bilateral tumors (LLC cells) were injected with either VT680-labeled wild-type phage (right) or VT680-labeled SPARC-targeted phage. Note the brightly fluorescent tumors in the near-infrared fluorescence channel of the SPARC-targeted phage clone [identical white light (WL) settings]. Reprinted with permission from ref 167. Copyright 2006 Neoplasia Press, Inc.
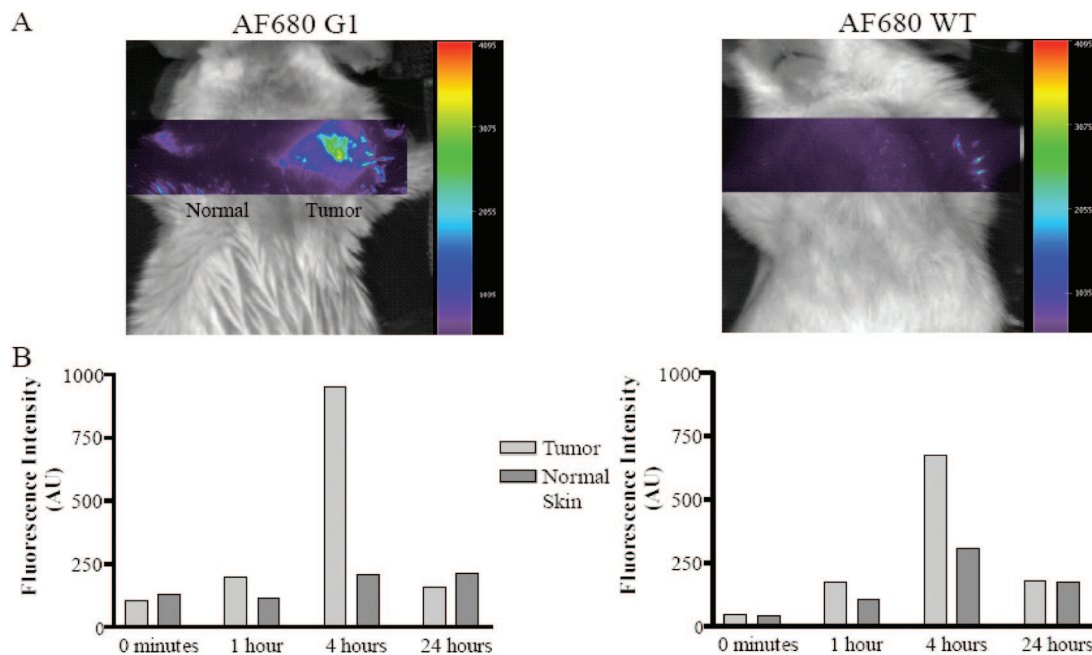


**Figure 10.** Optical imaging of prostate tumor-targeting phage in vivo. Phage displaying the prostate carcinoma-targeting peptide G1, IAGLATPGWSHWLAL (left top panel), labeled with AF680 were injected into the tail vein of PC-3 human prostate tumor xenografted mice. The animals were imaged 1, 4, and 24 h after phage injection. The only signal detected was from the tumor on the right shoulder of the mouse injected with prostate tumor-selected phage (blue image). Reprinted with permission from ref 119. Copyright 2006 Neoplasia Press, Inc.

forms. A benefit of the use of fluorescently labeled phage is that they can be used for long-term animal imaging studies, whereas radiolabeled phage may cause non-target-organ damage over long periods of time.

Numerous approaches have been undertaken to directly modify phage for use in optical imaging. The cpVIII of phage has been modified using standard chemistry approaches to obtain FITC-, AF647-, AF680-, and AF750-labeled phage that retain their target affinity.[165] K. Kelly et al. using intravital confocal microscopy demonstrated that phage displaying the VHSPNKK peptide (Table 1) imaged VCAM-1-expressing endothelial cells in a murine tumor necrosis factor-$\alpha$ (TNF$\alpha$) induced inflammatory ear model.[166] In another study from their group, phage that bound secreted

protein acidic and rich in cysteine (SPARC) upregulated in invasive cancer were obtained. Phage were selected against purified SPARC protein in vitro using a seven amino acid random linear peptide library (New England Biolaboratories, Cambridge MA). Clone 23, with the displayed peptide sequence SPPTGIN, was coupled using hydroxysuccinimide esters of VT680 and AF750 and used in surface reflectance imaging of Lewis lung carcinoma (LLC)-xenografted nude mice. The surface reflectance imaging (Figure 9) and fluorescent molecular tomography (FMT, not shown) clearly demonstrated increased tumor uptake compared with WT phage.[167]

In vivo selected phage that extravasate the vasculature and target tumors in vivo have been also used successfully in optical imaging. The ability of one such phage clone, G1 (Table 2), to image PC-3 tumors was investigated using AF680-labeled phage. The in vivo distribution of the G1 phage showed tumoral accumulation as early as 5 min and peaked from 4 to 6 h. To determine the usefulness of G1 phage as an in vivo imaging agent, surface reflectance imaging with AF680-labeled G1 phage was performed. AF680-labeled phage could be imaged in the PC-3 derived tumors in SCID mice as early as 1 h postinjection peaking at 4 h. At 4 h after injection of AF680 G1 phage, a 4.5-fold increase in the fluorescent signal within the tumor compared with that of the normal tissue was observed (Figure 10).[119]

## 7.3. Chimeric Phage and Nanoparticles

An intriguing application of phage is in the integration of tumor targeting and genetic (viral) imaging in order to deliver and image specific transgenes. Pasqualini, Arap, and co-workers developed chimeric phage (P) displaying the RGD-4C integrin-targeting sequence CDCRGDCFC and adeno-associated virus (AAV) constructs (AAVP vectors) which were evaluated for tumor targeting and imaging, and also herpes simplex virus thymidine kinase (HSVtk) gene expression in a mouse model of human soft-tissue sarcoma. PET imaging was performed with $^{18}$F-FDG and the nucleoside analogue 2′-$^{18}$F-fluoro-2″-deoxy-1-$\beta$-D-arabino-furanosyl-5-ethyl-uracil ($^{18}$F-FEAU), a substrate for HSVtk (Figure 11).[168,169] These studies demonstrated the simultaneous specific targeting of RGD-4C expressing cells, noninvasive imaging of HSVtk reporter genes, and drug response monitoring using a PET-based imaging probe. Further, these studies suggest that dual targeting AAV/phage vectors can be used to image gene expression and drug response prediction, which may be highly beneficial in humans.

Phage display selected peptides have also been conjugated to nanoparticles and used to image cancer. For example, Kelly et al. used phage display with cultured cells to identify peptides specific for pancreatic ductal adenocarcinoma (PDAC). Two clones, 15 (TMAPSIK) and 27 (LLPSGKP), demonstrated good affinity and specificity for the target PDAC cells. To test these plectin-1 binding peptides as potential diagnostic agents for PDAC, the phage were labeled with the fluorochromes VT680 and Texas Red then injected into mice from the Kras p53 PDAC model. This technique enabled the imaging of PDAC in mice. Peptide 27 was synthesized and attached to a magnetofluorescent nanoparticle (NP) (cross-linked iron oxide CLIO-Cy5.5, PTP-NP) and the resulting MRI/optical imaging agent was tested in PDAC tumor-bearing mice. Intravital confocal microscopy detected discrete areas of fluorescence in the abdomen of the mice 24 h after administration (Figure 12). Biodistribution
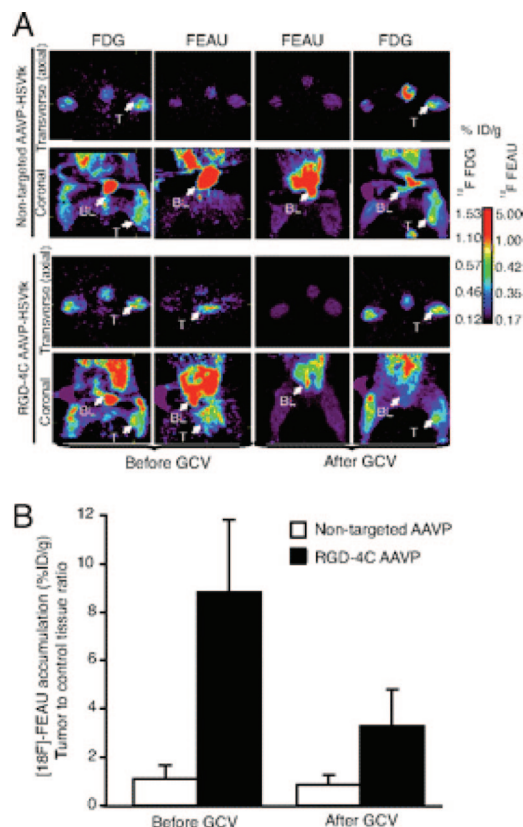


**Figure 11.** Predicting and monitoring drug response in a preclinical model of human sarcoma. PET imaging of HSVtk transgene expression was performed in sarcoma-bearing rats after iv delivery of RGD-4C targeted AAVP or nontargeted control. The first GCV treatment cycle was initiated at 24 h after [$^{18}$F]-FEAU administration and imaging to enable the molecular-genetic imaging of the corresponding drug response. (A) Cohorts of nude rats bearing human SKLMS1-derived xenografts ($n = 8$) received a single iv dose ($3 \times 10^{12}$ TU) of RGD-4C AAVP-HSVtk or control nontargeted AAVP-HSVtk. PET imaging of [$^{18}$F]-FEAU was performed after AAVP administration (day 9) and then again after drug treatment with GCV (day 15). PET imaging of [$^{18}$F]-FDG was performed on day 8 and then again after the second [$^{18}$F]-FEAU (day 16). PET imaging with [$^{18}$F]-FDG and with [$^{18}$F]-FEAU are presented (before and after treatment with GCV) as indicated. Transverse (axial) and coronal sections are shown. A standard calibration scale is provided, and correspondence of [$^{18}$F]-FDG and [$^{18}$F]-FEAU PET imaging is indicated. (B) Relative sarcoma expression of HSVtk as assessed by repetitive PET imaging with [$^{18}$F]-FEAU before and after initiation of cytotoxic drug treatment with GCV. A mesenchymal-derived normal tissue (muscle) served to normalize the tumor-to-control reporter transgene expression ratio. Reprinted with permission from ref 168. Copyright, 2008 National Academy of Sciences, U.S.A.

studies demonstrated specific uptake in tumor, with also some liver, kidney, spleen, and lung uptake. The agent was present in the tumor tissue rather than the vasculature since a vasculature agent administered before injection did not colocalize.[53]

## 8. Prospects and Challenges

Given the progress made in the past few years in utilizing phage display-selected peptides for the in vivo tumor imaging and diagnosis of cancer in animals, it is predicted that similar peptide constructs will be translated in the not too distant future into the clinic for use in humans. A major obstacle in efficacious use in humans is the high kidney uptake observed with radiolabeled peptides including those isolated using
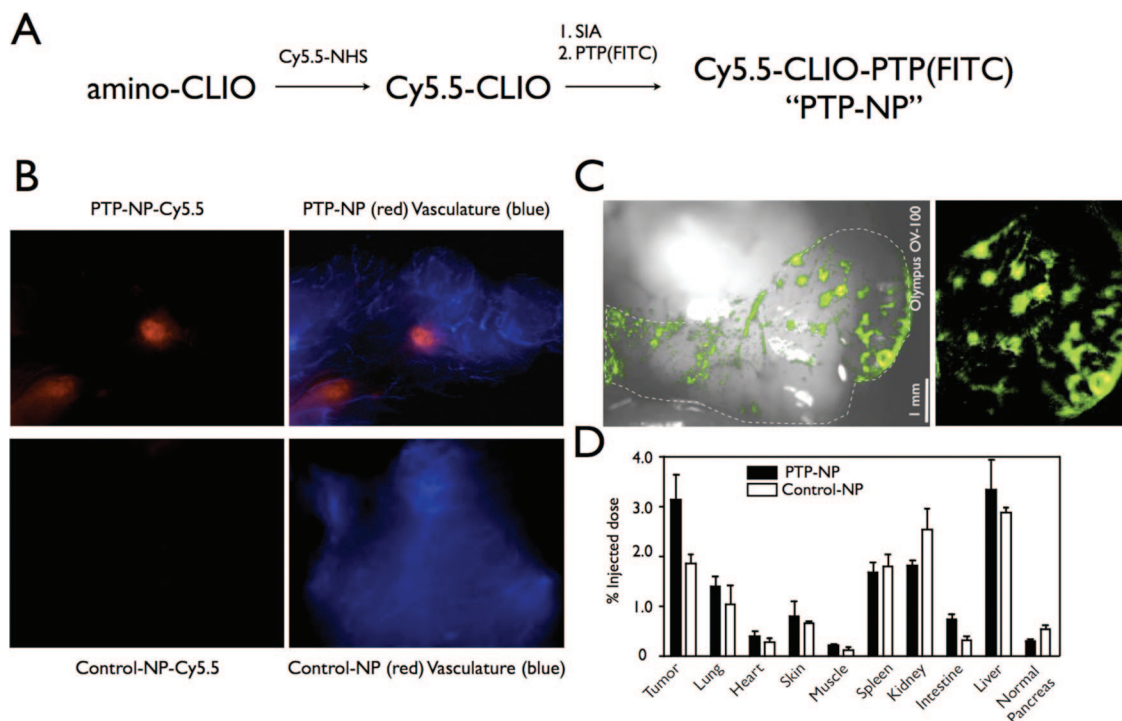
**Figure 12.** Fluorescence imaging of PDAC using PTP-NP or Control-NP. (A) Schematic of conjugation of PTP to NP. Control-NP is synthesized the same way with substitution of control peptide for PTP. (B) Intravital confocal microscopy of early pancreatic lesions imaged using PTP-NP (red, top) or control-NP (red, bottom) and AF750-labeled bloodpool agent (blue). (C) Low-magnification view of pancreatic fluorescence shows distribution of PTP-NP in distinct areas of the pancreas. White light overlay provides anatomic correlation (left). Dotted line outlines the pancreas. (D) Biodistribution of PTP-NP and control-NP. Reprinted with permission from ref 53. Copyright 2008 PLoS Medicine.

phage display.[154−156] Even though radiopharmaceutical renal clearance is preferred over elimination through the RES, high kidney uptake can severely limit the effectiveness of a radiolabeled peptide in diagnostic cancer imaging especially if the tumor (or metastases) is in the vicinity of the kidneys. A better understanding of the mechanisms of radiolabeled peptide renal retention in combination with novel molecular genetic and combinatorial approaches to identify peptide signatures retained in the kidney may be warranted. In addition to progress made with phage display-selected peptides, phage displaying the cancer-avid peptides have been utilized in vivo and are particularly well suited to a wide-range of modifications and imagining modalities. While their use in animals is gaining widespread acceptability, the use of phage in humans still faces obstacles including immunogenicity and clearance problems, especially because phage are extremely large and clear through the reticuloendothelial system. A combination of peptide and organic nanoparticle sciences may be an attractive approach to address some of the challenges.

## 9. Conclusion

Combinatorial chemistry and phage display technologies provide robust means for the rapid discovery of tumor antigen-avid peptides. By in vitro and in vivo phage display, new targeting peptides with capabilities to image tumors in living animals have been selected. In the last five years, many of these peptides have been radio or optically labeled for the imaging of a range of tumors in vivo. Phage bearing the tumor-avid peptide sequences have been modified so as to function as multimodal or multistep imaging agents, as well. Thus, phage display technology has developed into a rapid,

economical, and efficacious approach to the development of agents for the molecular imaging and diagnosis of cancer.

## 10. Abbreviations

| | |
|---|---|
| AAV | adeno-associated virus |
| AF | AlexaFluor |
| α-MSH | α-melanocyte stimulating hormone |
| CLIO | cross-linked iron oxide |
| cp | coat protein |
| CRIP-1 | cysteine-rich intestinal protein |
| DOTA | 1,4,7,10-tetraazacyclododecane-1,4,7,10-tetraacetic acid |
| DTPA | diethylenetriaminepentaacetic acid |
| EGFR | epidermal growth factor receptor |
| ECD | extracellular domain |
| FGF | fibroblast growth factor |
| ^{18}F-FDG | fluorine-18 2-deoxy-2-fluoro-D-glucose |
| ^{18}F-FEAU | 2′-^{18}F-fluoro-2″-deoxy-1-β-D-arabino-furanosyl-5-ethyl-uracil |
| FMT | fluorescent molecular tomography |
| GRP | gastrin releasing peptide |
| HSVtk | herpes simplex virus thymidine kinase |
| IGF-1 | insulin-like growth factor-1 |
| LLC | Lewis lung carcinoma |
| MMP | matrix metalloproteinase |
| NP | nanoparticle |
| NIRFs | near-infrared fluorophores |
| NSCLC | non-small-cell lung cancer |
| P | chimeric phage |
| PDAC | pancreatic ductal adenocarcinoma |
| PET | positron emission tomography |
| phage | bacteriophage |
| PBP | plectin-1 binding peptides |
| PSA | prostate specific antigen |

| Qdots | quantum dots |
|---|---|
| RES | reticuloendothelial system |
| SPARC | secreted protein acidic and rich in cysteine |
| SPECT | single-photon emission tomography |
| TAG-72 | tumor-associated glycoprotein 72 |
| TGF-$\beta$ | transforming growth factor-$\beta$ |
| TF | Thomsen−Friedenreich |
| TNF$\alpha$ | tumor necrosis factor-$\alpha$ |
| uPA | urokinase plasminogen activator |
| uPAR | urokinase plasminogen activator receptor |
| VCAM-1 | vascular cell adhesion molecule-1-targeting |
| VEGF | vascular endothelial growth factor |

## 11. Acknowledgments

## 12. References

(1) Hood, L.; Heath, J. R.; Phelps, M. E.; Lin, B. *Science* **2004**, *306*, 640.
(2) Rudin, M.; Weissleder, R. *Nat. Rev. Drug Discovery* **2003**, *2*, 123.
(3) Akerman, M. E.; Chan, W. C.; Laakkonen, P.; Bhatia, S. N.; Ruoslahti, E. *Proc. Natl. Acad. Sci. U.S.A.* **2002**, *99*, 12617.
(4) Kelly, K. A.; Jones, D. A. *Neoplasia* **2003**, *5*, 437.
(5) Glinsky, V. V.; Glinsky, G. V.; Rittenhouse-Olson, K.; Huflejt, M. E.; Glinskii, O. V.; Deutscher, S. L.; Quinn, T. P. *Cancer Res.* **2001**, *61*, 4851.
(6) Glinsky, V. V.; Glinsky, G. V.; Glinskii, O. V.; Huxley, V. H.; Turk, J. R.; Mossine, V. V.; Deutscher, S. L.; Pienta, K. J.; Quinn, T. P. *Cancer Res.* **2003**, *63*, 3805.
(7) Pierce, M. C.; Javier, D. J.; Richards-Kortum, R. *Int. J. Cancer* **2008**, *123*, 1979.
(8) Ray, P.; Wu, A. M.; Gambhir, S. S. *Cancer Res.* **2003**, *63*, 1160.
(9) Edwards, W. B.; Xu, B.; Akers, W.; Cheney, P. P.; Liang, K.; Rogers, B. E.; Anderson, C. J.; Achilefu, S. *Bioconjugate Chem.* **2008**, *19*, 192.
(10) Sharkey, R. M.; Goldenberg, D. M. *J. Nucl. Med.* **2005**, *46* (Suppl. 1), 115S.
(11) Kruglyak, E.; Freeman, L. M.; Wadler, S. *Ann. Oncol.* **1997**, *8*, 301.
(12) Goldenberg, M. M. *Clin. Ther.* **1999**, *21*, 309.
(13) Klastersky, J. *Curr. Opin. Oncol.* **2006**, *18*, 316.
(14) Goldenberg, D. M. *J. Nucl. Med.* **2002**, *43*, 693.
(15) Lewis, M. R.; Wang, M.; Axworthy, D. B.; Theodore, L. J.; Mallet, R. W.; Fritzberg, A. R.; Welch, M. J.; Anderson, C. J. *J. Nucl. Med.* **2003**, *44*, 1284.
(16) Reubi, J. C. *Endocr. Rev.* **2003**, *24*, 389.
(17) Behr, T. M.; Gotthardt, M.; Barth, A.; Behe, M. Q. *J. Nucl. Med.* **2001**, *45*, 189.
(18) Bakker, W. H.; Krenning, E. P.; Reubi, J. C.; Breeman, W. A.; Setyono-Han, B.; de Jong, M.; Kooij, P. P.; Bruns, C.; van Hagen, P. M.; Marbach, P. *Life Sci.* **1991**, *49*, 1593.
(19) Smith, C. J.; Volkert, W. A.; Hoffman, T. J. *Nucl. Med. Biol.* **2003**, *30*, 861.
(20) Chen, J.; Cheng, Z.; Miao, Y.; Jurisson, S. S.; Quinn, T. P. *Cancer* **2002**, *94*, 1196.
(21) Miao, Y.; Owen, N. K.; Fisher, D. R.; Hoffman, T. J.; Quinn, T. P. *J. Nucl. Med.* **2005**, *46*, 121.
(22) Chen, J.; Cheng, Z.; Hoffman, T. J.; Jurisson, S. S.; Quinn, T. P. *Cancer Res.* **2000**, *60*, 5649.
(23) Chen, J.; Cheng, Z.; Owen, N. K.; Hoffman, T. J.; Miao, Y.; Jurisson, S. S.; Quinn, T. P. *J. Nucl. Med.* **2001**, *42*, 1847.
(24) Miao, Y.; Benwell, K.; Quinn, T. P. *J. Nucl. Med.* **2007**, *48*, 73.
(25) Miao, Y.; Hylarides, M.; Fisher, D. R.; Shelton, T.; Moore, H.; Wester, D. W.; Fritzberg, A. R.; Winkelmann, C. T.; Hoffman, T.; Quinn, T. P. *Clin. Cancer Res.* **2005**, *11*, 5616.
(26) Wei, L.; Miao, Y.; Gallazzi, F.; Quinn, T. P.; Welch, M. J.; Vavere, A. L.; Lewis, J. S. *Nucl. Med. Biol.* **2007**, *34*, 945.
(27) McQuade, P.; Miao, Y.; Yoo, J.; Quinn, T. P.; Welch, M. J.; Lewis, J. S. *J. Med. Chem.* **2005**, *48*, 2985.
(28) Houghten, R. A.; Pinilla, C.; Blondelle, S. E.; Appel, J. R.; Dooley, C. T.; Cuervo, J. H. *Nature* **1991**, *354*, 84.
(29) Smith, G. P. *Science* **1985**, *228*, 1315.
(30) Atwell, S.; Wells, J. A. *Proc. Natl. Acad. Sci. U.S.A.* **1999**, *96*, 9497.

(31) Barbas, C. F.; Kang, A. S.; Lerner, R. A.; Benkovic, S. J. *Proc. Natl. Acad. Sci. U.S.A.* **1991**, *88*, 7978.
(32) Smith, G. P.; Petrenko, V. A. *Chem. Rev.* **1997**, *97*, 391.
(33) Brissette, R.; Goldstein, N. I. *Methods Mol. Biol.* **2007**, *383*, 203.
(34) Bessette, P. H.; Rice, J. J.; Daugherty, P. S. *Protein Eng., Des. Sel.* **2004**, *17*, 731.
(35) Lunder, M.; Bratkovic, T.; Urleb, U.; Kreft, S.; Strukelj, B. *Biotechniques* **2008**, *44*, 893.
(36) Noppe, W.; Plieva, F.; Galaev, I. Y.; Pottel, H.; Deckmyn, H.; Mattiasson, B. *BMC Biotechnol.* **2009**, *9*, 21.
(37) Liu, Y.; Adams, J. D.; Turner, K.; Cochran, F. V.; Gambhir, S. S.; Soh, H. T. *Lab Chip* **2009**, *9*, 1033.
(38) Yip, Y. L.; Ward, R. L. *Curr. Pharm. Biotechnol.* **2002**, *3*, 29.
(39) Brown, K. C. *Curr. Opin. Chem. Biol.* **2000**, *4*, 16.
(40) Aina, O. H.; Sroka, T. C.; Chen, M. L.; Lam, K. S. *Biopolymers.* **2002**, *66*, 184.
(41) Sehgal, A. *Curr. Opin. Drug Discovery Dev.* **2002**, *5*, 245.
(42) Work, L. M.; Nicklin, S. A.; White, S. J.; Baker, A. H. *Methods Enzymol.* **2002**, *346*, 157.
(43) Ladner, R. C. Q. *J. Nucl. Med.* **1999**, *43*, 119.
(44) Hoess, R. H. *Chem. Rev.* **2001**, *101*, 3205.
(45) Nilsson, F.; Tarli, L.; Viti, F.; Neri, D. *Adv. Drug Delivery Rev.* **2000**, *43*, 165.
(46) Manoutcharian, K.; Gevorkian, G.; Cano, A.; Almagro, J. C. *Curr. Pharm. Biotechnol.* **2001**, *2*, 217.
(47) Nielsen, U. B.; Marks, J. D. *Pharm. Sci. Technol. Today* **2000**, *3*, 282.
(48) Skelton, N. J.; Chen, Y. M.; Dubree, N.; Quan, C.; Jackson, D. Y.; Cochran, A.; Zobel, K.; Deshayes, K.; Baca, M.; Pisabarro, M. T.; Lowman, H. B. *Biochemistry* **2001**, *40*, 8487.
(49) Peletskaya, E. N.; Glinsky, V. V.; Glinsky, G. V.; Deutscher, S. L.; Quinn, T. P. *J. Mol. Biol.* **1997**, *270*, 374.
(50) Kelly, K. A.; Nahrendorf, M.; Yu, A. M.; Reynolds, F.; Weissleder, R. *Mol. Imaging Biol.* **2006**, *8*, 201.
(51) Fukuda, M. N.; Ohyama, C.; Lowitz, K.; Matsuo, O.; Pasqualini, R.; Ruoslahti, E.; Fukuda, M. *Cancer Res.* **2000**, *60*, 450.
(52) Funovics, M.; Montet, X.; Reynolds, F.; Weissleder, R.; Josephson, L. *Neoplasia* **2005**, *7*, 904.
(53) Kelly, K. A.; Bardeesy, N.; Anbazhagan, R.; Gurumurthy, S.; Berger, J.; Alencar, H.; Depinho, R. A.; Mahmood, U.; Weissleder, R. *PLoS Med.* **2008**, *5*, e85.
(54) Kelly, K. A.; Setlur, S. R.; Ross, R.; Anbazhagan, R.; Waterman, P.; Rubin, M. A.; Weissleder, R. *Cancer Res.* **2008**, *68*, 2286.
(55) Kumar, S. R.; Quinn, T. P.; Deutscher, S. L. *Clin. Cancer Res.* **2007**, *13*, 6070.
(56) Thapa, N.; Kim, S.; So, I. S.; Lee, B. H.; Kwon, I. C.; Choi, K.; Kim, I. S. *J. Cell. Mol. Med.* **2008**, *12*, 1649.
(57) Witt, H.; Hajdin, K.; Iljin, K.; Greiner, O.; Niggli, F. K.; Schafer, B. W.; Bernasconi, M. *Int. J. Cancer* **2009**, *124*, 2026.
(58) Fusenig, N. E.; Boukamp, P. *Mol. Carcinog.* **1998**, *23*, 144.
(59) Zhu, Z. Y.; Zhong, C. P.; Xu, W. F.; Lin, G. M.; Ye, G. Q.; Ji, Y. Y.; Sun, B.; Yeh, M. *Cell Res.* **1999**, *9*, 271.
(60) Riemer, A. B.; Jensen-Jarolim, E. *Immunol. Lett.* **2007**, *113*, 1.
(61) Riemer, A. B.; Klinger, M.; Wagner, S.; Bernhaus, A.; Mazzucchelli, L.; Pehamberger, H.; Scheiner, O.; Zielinski, C. C.; Jensen-Jarolim, E. *J. Immunol.* **2004**, *173*, 394.
(62) Hao, J.; Serohijos, A. W.; Newton, G.; Tassone, G.; Wang, Z.; Sgroi, D. C.; Dokholyan, N. V.; Basilion, J. P. *PLoS Comput. Biol.* **2008**, *4*, e1000138.
(63) Koolpe, M.; Burgess, R.; Dail, M.; Pasquale, E. B. *J. Biol. Chem.* **2005**, *280*, 17301.
(64) Koolpe, M.; Dail, M.; Pasquale, E. B. *J. Biol. Chem.* **2002**, *277*, 46974.
(65) Kim, Y.; Lillo, A. M.; Steiniger, S. C.; Liu, Y.; Ballatore, C.; Anichini, A.; Mortarini, R.; Kaufmann, G. F.; Zhou, B.; Felding-Habermann, B.; Janda, K. D. *Biochemistry* **2006**, *45*, 9434.
(66) Vidal, C. I.; Mintz, P. J.; Lu, K.; Ellis, L. M.; Manenti, L.; Giavazzi, R.; Gershenson, D. M.; Broaddus, R.; Liu, J.; Arap, W.; Pasqualini, R. *Oncogene* **2004**, *23*, 8859.
(67) Pazgier, M.; Liu, M.; Zou, G.; Yuan, W.; Li, C.; Li, J.; Monbo, J.; Zella, D.; Tarasov, S. G.; Lu, W. *Proc. Natl. Acad. Sci. U.S.A.* **2009**, *106*, 4665.
(68) Zurita, A. J.; Troncoso, P.; Cardo-Vila, M.; Logothetis, C. J.; Pasqualini, R.; Arap, W. *Cancer Res.* **2004**, *64*, 435.
(69) Pakkala, M.; Jylhasalmi, A.; Wu, P.; Leinonen, J.; Stenman, U. H.; Santa, H.; Vepsalainen, J.; Perakyla, M.; Narvanen, A. *J. Pept. Sci.* **2004**, *10*, 439.
(70) Zhao, X.; Hu, J.; Huang, R.; Yang, L. *J. Exp. Clin. Cancer Res.* **2007**, *26*, 509.
(71) Jager, S.; Jahnke, A.; Wilmes, T.; Adebahr, S.; Vogtle, F. N.; Delima-Hahn, E.; Pfeifer, D.; Berg, T.; Lubbert, M.; Trepel, M. *Leukemia* **2007**, *21*, 411.

(72) Hetian, L.; Ping, A.; Shumei, S.; Xiaoying, L.; Luowen, H.; Jian, W.; Lin, M.; Meisheng, L.; Junshan, Y.; Chengchao, S. *J. Biol. Chem.* **2002**, *277*, 43137.

(73) Fan, H.; Duan, Y.; Zhou, H.; Li, W.; Li, F.; Guo, L.; Roeske, R. W. *IUBMB Life* **2002**, *54*, 67.

(74) Maruta, F.; Parker, A. L.; Fisher, K. D.; Hallissey, M. T.; Ismail, T.; Rowlands, D. C.; Chandler, L. A.; Kerr, D. J.; Seymour, L. W. *Cancer Gene Ther.* **2002**, *9*, 543.

(75) Binetruy-Tournaire, R.; Demangel, C.; Malavaud, B.; Vassy, R.; Rouyre, S.; Kraemer, M.; Plouet, J.; Derbin, C.; Perret, G.; Mazie, J. C. *EMBO J.* **2000**, *19*, 1525.

(76) Michon, I. N.; Penning, L. C.; Molenaar, T. J.; van Berkel, T. J.; Biessen, E. A.; Kuiper, J. *Biochem. Biophys. Res. Commun.* **2002**, *293*, 1279.

(77) Hyun, S.; Lee, E. H.; Park, J.; Yu, J. *Bioorg. Med. Chem. Lett.* **2008**, *18*, 4011.

(78) Peletskaya, E. N.; Glinsky, G.; Deutscher, S. L.; Quinn, T. P. *Mol. Diversity* **1996**, *2*, 13.

(79) Glinsky, V. V.; Huflejt, M. E.; Glinsky, G. V.; Deutscher, S. L.; Quinn, T. P. *Cancer Res.* **2000**, *60*, 2584.

(80) Landon, L. A.; Peletskaya, E. N.; Glinsky, V. V.; Karasseva, N.; Quinn, T. P.; Deutscher, S. L. *J. Protein Chem.* **2003**, *22*, 193.

(81) Landon, L. A.; Zou, J.; Deutscher, S. L. *Mol. Diversity* **2003**, *8*, 35.

(82) Kubo, N.; Akita, N.; Shimizu, A.; Kitahara, H.; Parker, A. L.; Miyagawa, S. *J. Drug Targeting* **2008**, *16*, 396.

(83) Ding, H.; Prodinger, W. M.; Kopecek, J. *Bioconjugate Chem.* **2006**, *17*, 514.

(84) McGuire, M. J.; Samli, K. N.; Chang, Y. C.; Brown, K. C. *Exp. Hematol.* **2006**, *34*, 443.

(85) Choi, J. H.; Lee, W. K.; Han, S. H.; Ha, S.; Ahn, S. M.; Kang, J. S.; Choi, Y. J.; Yun, C. H. *Int. Immunopharmacol.* **2008**, *8*, 852.

(86) Askoxylakis, V.; Zitzmann, S.; Mier, W.; Graham, K.; Kramer, S.; von Wegner, F.; Fink, R. H.; Schwab, M.; Eisenhut, M.; Haberkorn, U. *Clin. Cancer Res.* **2005**, *11*, 6705.

(87) Robinson, P.; Stuber, D.; Deryckere, F.; Tedbury, P.; Lagrange, M.; Orfanoudakis, G. *J. Mol. Recognit.* **2005**, *18*, 175.

(88) Rasmussen, U. B.; Schreiber, V.; Schultz, H.; Mischler, F.; Schughart, K. *Cancer Gene Ther.* **2002**, *9*, 606.

(89) Zhang, Y.; Chen, J.; Hu, Z.; Hu, D.; Pan, Y.; Ou, S.; Liu, G.; Yin, X.; Zhao, J.; Ren, L.; Wang, J. *J. Biomol. Screening* **2007**, *12*, 429.

(90) Liang, S.; Lin, T.; Ding, J.; Pan, Y.; Dang, D.; Guo, C.; Zhi, M.; Zhao, P.; Sun, L.; Hong, L.; Shi, Y.; Yao, L.; Liu, J.; Wu, K.; Fan, D. *J. Mol. Med.* **2006**, *84*, 764.

(91) Wu, C.; Lo, S. L.; Boulaire, J.; Hong, M. L.; Beh, H. M.; Leung, D. S.; Wang, S. *J. Controlled Release* **2008**, *130*, 140.

(92) Du, B.; Qian, M.; Zhou, Z.; Wang, P.; Wang, L.; Zhang, X.; Wu, M.; Zhang, P.; Mei, B. *Biochem. Biophys. Res. Commun.* **2006**, *342*, 956.

(93) Zang, L.; Shi, L.; Guo, J.; Pan, Q.; Wu, W.; Pan, X.; Wang, J. *Cancer Lett.* **2009**, *281*, 64.

(94) Chang, D. K.; Lin, C. T.; Wu, C. H.; Wu, H. C. *PLoS One* **2009**, *4*, e4171.

(95) Askoxylakis, V.; Mier, W.; Zitzmann, S.; Ehemann, V.; Zhang, J.; Kramer, S.; Beck, C.; Schwab, M.; Eisenhut, M.; Haberkorn, U. *J. Nucl. Med.* **2006**, *47*, 981.

(96) Romanov, V. I.; Durand, D. B.; Petrenko, V. A. *Prostate* **2001**, *47*, 239.

(97) Zitzmann, S.; Mier, W.; Schad, A.; Kinscherf, R.; Askoxylakis, V.; Kramer, S.; Altmann, A.; Eisenhut, M.; Haberkorn, U. *Clin. Cancer Res.* **2005**, *11*, 139.

(98) Zitzmann, S.; Kramer, S.; Mier, W.; Hebling, U.; Altmann, A.; Rother, A.; Berndorff, D.; Eisenhut, M.; Haberkorn, U. *J. Nucl. Med.* **2007**, *48*, 965.

(99) Pasqualini, R.; Ruoslahti, E. *Nature* **1996**, *380*, 364.

(100) Arap, W.; Kolonin, M.; Trepel, M.; Lahdenranta, J.; Cardo-Vila, M.; Giordano, R. J.; Mintz, P. J.; Ardelt, P. U.; Yao, V. J.; Vidal, C. I.; Chen, L.; Flamm, A.; Valtanen, H.; Weavind, L. M.; Hicks, M. E.; Pollock, R. E.; Botz, G. H.; Bucana, C. D.; Koivunen, E.; Cahill, D.; Troncoso, P.; Baggerly, K. A.; Pentz, R. D.; Do, K. A.; Logothetis, C. J.; Pasqualini, R. *Nat. Med.* **2002**, *8*, 121.

(101) Arap, W.; Haedicke, W.; Bernasconi, M.; Kain, R.; Rajotte, D.; Krajewski, S.; Ellerby, H. M.; Bredesen, D. E.; Pasqualini, R.; Ruoslahti, E. *Proc. Natl. Acad. Sci. U.S.A.* **2002**, *99*, 1527.

(102) Kolonin, M. G.; Bover, L.; Sun, J.; Zurita, A. J.; Do, K. A.; Lahdenranta, J.; Cardo-Vila, M.; Giordano, R. J.; Jaalouk, D. E.; Ozawa, M. G.; Moya, C. A.; Souza, G. R.; Staquicini, F. I.; Kunyiasu, A.; Scudiero, D.; Holbeck, S. L.; Sausville, E. A.; Arap, W.; Pasqualini, R. *Cancer Res.* **2006**, *66*, 34.

(103) Nishimura, S.; Takahashi, S.; Kamikatahira, H.; Kuroki, Y.; Jaalouk, D. E.; O'Brien, S.; Koivunen, E.; Arap, W.; Pasqualini, R.; Nakayama, H.; Kuniyasu, A. *J. Biol. Chem.* **2008**, *283*, 11752.

(104) Arap, W.; Pasqualini, R.; Ruoslahti, E. *Science* **1998**, *279*, 377.

(105) Cai, W.; Shin, D. W.; Chen, K.; Gheysens, O.; Cao, Q.; Wang, S. X.; Gambhir, S. S.; Chen, X. *Nano Lett.* **2006**, *6*, 669.

(106) Chen, X.; Sievers, E.; Hou, Y.; Park, R.; Tohme, M.; Bart, R.; Bremner, R.; Bading, J. R.; Conti, P. S. *Neoplasia* **2005**, *7*, 271.

(107) Cheng, Z.; Wu, Y.; Xiong, Z.; Gambhir, S. S.; Chen, X. *Bioconjugate Chem.* **2005**, *16*, 1433.

(108) Haubner, R.; Wester, H. J. *Curr. Pharm. Des.* **2004**, *10*, 1439.

(109) Kwon, S.; Ke, S.; Houston, J. P.; Wang, W.; Wu, Q.; Li, C.; Sevick-Muraca, E. M. *Mol. Imaging* **2005**, *4*, 75.

(110) Su, Z. F.; Liu, G.; Gupta, S.; Zhu, Z.; Rusckowski, M.; Hnatowich, D. J. *Bioconjugate Chem.* **2002**, *13*, 561.

(111) Wang, W.; Ke, S.; Wu, Q.; Charnsangavej, C.; Gurfinkel, M.; Gelovani, J. G.; Abbruzzese, J. L.; Sevick-Muraca, E. M.; Li, C. *Mol. Imaging* **2004**, *3*, 343.

(112) Ye, Y.; Bloch, S.; Xu, B.; Achilefu, S. *J. Med. Chem.* **2006**, *49*, 2268.

(113) Laakkonen, P.; Zhang, L.; Ruoslahti, E. *Ann. N.Y. Acad. Sci.* **2008**, *1131*, 37.

(114) Essler, M.; Ruoslahti, E. *Proc. Natl. Acad. Sci. U.S.A.* **2002**, *99*, 2252.

(115) Yao, V. J.; Ozawa, M. G.; Trepel, M.; Arap, W.; McDonald, D. M.; Pasqualini, R. *Am. J. Pathol.* **2005**, *166*, 625.

(116) Sato, M.; Arap, W.; Pasqualini, R. *Oncology* **2007**, *21*, 1346.

(117) Newton, J.; Deutscher, S. L. *Handb. Exp. Pharmacol.* **2008**, 145.

(118) Newton, J. R.; Deutscher, S. L. *Methods Mol. Biol.* **2009**, *504*, 275.

(119) Newton, J. R.; Kelly, K. A.; Mahmood, U.; Weissleder, R.; Deutscher, S. L. *Neoplasia* **2006**, *8*, 772.

(120) Zou, J.; Dickerson, M. T.; Owen, N. K.; Landon, L. A.; Deutscher, S. L. *Mol. Biol. Rep.* **2004**, *31*, 121.

(121) Margulies, M.; Egholm, M.; Altman, W. E.; Attiya, S.; Bader, J. S.; Bemben, L. A.; Berka, J.; Braverman, M. S.; Chen, Y. J.; Chen, Z.; Dewell, S. B.; Du, L.; Fierro, J. M.; Gomes, X. V.; Godwin, B. C.; He, W.; Helgesen, S.; Ho, C. H.; Irzyk, G. P.; Jando, S. C.; Alenquer, M. L.; Jarvie, T. P.; Jirage, K. B.; Kim, J. B.; Knight, J. R.; Lanza, J. R.; Leamon, J. H.; Lefkowitz, S. M.; Lei, M.; Li, J.; Lohman, K. L.; Lu, H.; Makhijani, V. B.; McDade, K. E.; McKenna, M. P.; Myers, E. W.; Nickerson, E.; Nobile, J. R.; Plant, R.; Puc, B. P.; Ronan, M. T.; Roth, G. T.; Sarkis, G. J.; Simons, J. F.; Simpson, J. W.; Srinivasan, M.; Tartaro, K. R.; Tomasz, A.; Vogt, K. A.; Volkmer, G. A.; Wang, S. H.; Wang, Y.; Weiner, M. P.; Yu, P.; Begley, R. F.; Rothberg, J. M. *Nature* **2005**, *437*, 376.

(122) Porreca, G. J.; Zhang, K.; Li, J. B.; Xie, B.; Austin, D.; Vassallo, S. L.; LeProust, E. M.; Peck, B. J.; Emig, C. J.; Dahl, F.; Gao, Y.; Church, G. M.; Shendure, J. *Nat. Methods* **2007**, *4*, 931.

(123) Jurisson, S. S.; Lydon, J. D. *Chem. Rev.* **1999**, *99*, 2205.

(124) Bourguignon, M. H.; Loc'h, G.; Maziere, B. *J. Nucl. Biol. Med.* **1994**, *38*, 573.

(125) Mindt, T. L.; Struthers, H.; Brans, L.; Anguelov, T.; Schweinsberg, C.; Maes, V.; Tourwe, D.; Schibli, R. *J. Am. Chem. Soc.* **2006**, *128*, 15096.

(126) Anderson, C. J.; Welch, M. J. *Chem. Rev.* **1999**, *99*, 2219.

(127) Adler, L. P.; Crowe, J. P.; al-Kaisi, N. K.; Sunshine, J. L. *Radiology* **1993**, *187*, 743.

(128) Pelosi, E.; Messa, C.; Sironi, S.; Picchio, M.; Landoni, C.; Bettinardi, V.; Gianolli, L.; Del Maschio, A.; Gilardi, M. C.; Fazio, F. *Eur. J. Nucl. Med. Mol. Imaging* **2004**, *31*, 932.

(129) McCarthy, D. W.; Shefer, R. E.; Klinkowstein, R. E.; Bass, L. A.; Margeneau, W. H.; Cutler, C. S.; Anderson, C. J.; Welch, M. J. *Nucl. Med. Biol.* **1997**, *24*, 35.

(130) Zhernosekov, K. P.; Filosofov, D. V.; Baum, R. P.; Aschoff, P.; Bihl, H.; Razbash, A. A.; Jahn, M.; Jennewein, M.; Rosch, F. *J. Nucl. Med.* **2007**, *48*, 1741.

(131) Breeman, W. A.; Verbruggen, A. M. *Eur. J. Nucl. Med. Mol. Imaging* **2007**, *34*, 978.

(132) Doyle, T. C.; Burns, S. M.; Contag, C. H. *Cell. Microbiol.* **2004**, *6*, 303.

(133) Shaner, N. C.; Campbell, R. E.; Steinbach, P. A.; Giepmans, B. N.; Palmer, A. E.; Tsien, R. Y. *Nat. Biotechnol.* **2004**, *22*, 1567.

(134) Ballou, B.; Lagerholm, B. C.; Ernst, L. A.; Bruchez, M. P.; Waggoner, A. S. *Bioconjugate Chem.* **2004**, *15*, 79.

(135) Li, C.; Greenwood, T. R.; Glunde, K. *Neoplasia* **2008**, *10*, 389.

(136) Kovar, J. L.; Volcheck, W.; Sevick-Muraca, E.; Simpson, M. A.; Olive, D. M. *Anal. Biochem.* **2009**, *384*, 254.

(137) Sampath, L.; Kwon, S.; Ke, S.; Wang, W.; Schiff, R.; Mawad, M. E.; Sevick-Muraca, E. M. *J. Nucl. Med.* **2007**, *48*, 1501.

(138) Culver, J.; Akers, W.; Achilefu, S. *J. Nucl. Med.* **2008**, *49*, 169.

(139) Li, C.; Wang, W.; Wu, Q.; Ke, S.; Houston, J.; Sevick-Muraca, E.; Dong, L.; Chow, D.; Charnsangavej, C.; Gelovani, J. G. *Nucl. Med. Biol.* **2006**, *33*, 349.

(140) Hui, X.; Han, Y.; Liang, S.; Liu, Z.; Liu, J.; Hong, L.; Zhao, L.; He, L.; Cao, S.; Chen, B.; Yan, K.; Jin, B.; Chai, N.; Wang, J.; Wu, K.; Fan, D. *J. Controlled Release* **2008**, *131*, 86.

(141) Kuhnast, B.; Bodenstein, C.; Haubner, R.; Wester, H. J.; Senekowitsch-Schmidtke, R.; Schwaiger, M.; Weber, W. A. *Nucl. Med. Biol.* **2004**, *31*, 337.

(142) Chen, J.; Tung, C. H.; Allport, J. R.; Chen, S.; Weissleder, R.; Huang, P. L. *Circulation* **2005**, *111*, 1800.

(143) Ploug, M.; Østergaard, S.; Gårdsvoll, H.; Kovalski, K.; Holst-Hansen, C.; Holm, A.; Ossowski, L.; Danø, K. *Biochemistry* **2001**, *40*, 12157.

(144) Goodson, R. J.; Doyle, M. V.; Kaufman, S. E.; Rosenberg, S. *Proc. Natl. Acad. Sci. U.S.A.* **1994**, *91*, 7129.

(145) Li, Z. B.; Niu, G.; Wang, H.; He, L.; Yang, L.; Ploug, M.; Chen, X. *Clin. Cancer Res.* **2008**, *14*, 4758.

(146) Karasseva, N.; Glinsky, V. V.; Chen, N. X.; Komatireddy, R.; Quinn, T. P. *J. Protein Chem.* **2002**, *21*, 287.

(147) Howell, R. C.; Revskaya, E.; Pazo, V.; Nosanchuk, J. D.; Casadevall, A.; Dadachova, E. *Bioconjugate Chem.* **2007**, *18*, 1739.

(148) Zou, J.; Glinsky, V. V.; Landon, L. A.; Matthews, L.; Deutscher, S. L. *Carcinogenesis* **2005**, *26*, 309.

(149) Kumar, S. R.; Deutscher, S. L. *J. Nucl. Med.* **2008**, *49*, 796.

(150) Landgraf, R. *Breast Cancer Res.* **2007**, *9*, 202.

(151) Holbro, T.; Hynes, N. E. *Annu. Rev. Pharmacol. Toxicol.* **2004**, *44*, 195.

(152) Lub-de Hooge, M. N.; Kosterink, J. G.; Perik, P. J.; Nijnuis, H.; Tran, L.; Bart, J.; Suurmeijer, A. J.; de Jong, S.; Jager, P. L.; de Vries, E. G. *Br. J. Pharmacol.* **2004**, *143*, 99.

(153) Tolmachev, V.; Orlova, A.; Pehrson, R.; Galli, J.; Baastrup, B.; Andersson, K.; Sandstrom, M.; Rosik, D.; Carlsson, J.; Lundqvist, H.; Wennborg, A.; Nilsson, F. Y. *Cancer Res.* **2007**, *67*, 2773.

(154) Garcia Garayoa, E.; Ruegg, D.; Blauenstein, P.; Zwimpfer, M.; Khan, I. U.; Maes, V.; Blanc, A.; Beck-Sickinger, A. G.; Tourwe, D. A.; Schubiger, P. A. *Nucl. Med. Biol.* **2007**, *34*, 17.

(155) Behr, T. M.; Sharkey, R. M.; Juweid, M. E.; Blumenthal, R. D.; Dunn, R. M.; Griffiths, G. L.; Bair, H. J.; Wolf, F. G.; Becker, W. S.; Goldenberg, D. M. *Cancer Res.* **1995**, *55*, 3825.

(156) Rolleman, E. J.; Valkema, R.; de Jong, M.; Kooij, P. P.; Krenning, E. P. *Eur. J. Nucl. Med. Mol. Imaging* **2003**, *30*, 9.

(157) Racusen, L. C.; Whelton, A.; Solez, K. *Am. J. Pathol.* **1985**, *120*, 436.

(158) Mogensen, C. E. *Scand. J. Clin. Lab. Invest* **1977**, *37*, 477 Solling.

(159) van Eerd, J. E.; Vegt, E.; Wetzels, J. F.; Russel, F. G.; Masereeuw, R.; Corstens, F. H.; Oyen, W. J.; Boerman, O. C. *J. Nucl. Med.* **2006**, *47*, 528.

(160) Perea, S. E.; Reyes, O.; Baladron, I.; Perera, Y.; Farina, H.; Gil, J.; Rodriguez, A.; Bacardi, D.; Marcelo, J. L.; Cosme, K.; Cruz, M.; Valenzuela, C.; Lopez-Saura, P. A.; Puchades, Y.; Serrano, J. M.; Mendoza, O.; Castellanos, L.; Sanchez, A.; Betancourt, L.; Besada, V.; Silva, R.; Lopez, E.; Falcon, V.; Hernandez, I.; Solares, M.; Santana, A.; Diaz, A.; Ramos, T.; Lopez, C.; Ariosa, J.; Gonzalez, L. J.; Garay, H.; Gomez, D.; Gomez, R.; Alonso, D. F.; Sigman, H.; Herrera, L.; Acevedo, B. *Mol. Cell. Biochem.* **2008**, *316*, 163.

(161) Rusckowski, M.; Gupta, S.; Liu, G.; Dou, S.; Hnatowich, D. J. *J. Nucl. Med.* **2004**, *45*, 1201.

(162) Rusckowski, M.; Gupta, S.; Liu, G.; Dou, S.; Hnatowich, D. J. *Nucl. Med. Biol.* **2008**, *35*, 433.

(163) Newton, J. R.; Miao, Y.; Deutscher, S. L.; Quinn, T. P. *J. Nucl. Med.* **2007**, *48*, 429.

(164) Newton-Northup, J. R.; Figueroa, S. D.; Quinn, T. P.; Deutscher, S. L. *Nucl. Med. Biol.* **2009**, *36*, 789.

(165) Jaye, D. L.; Geigerman, C. M.; Fuller, R. E.; Akyildiz, A.; Parkos, C. A. *J. Immunol. Methods* **2004**, *295*, 119.

(166) Kelly, K. A.; Clemons, P. A.; Yu, A. M.; Weissleder, R. *Mol. Imaging* **2006**, *5*, 24.

(167) Kelly, K. A.; Waterman, P.; Weissleder, R. *Neoplasia* **2006**, *8*, 1011.

(168) Hajitou, A.; Lev, D. C.; Hannay, J. A.; Korchin, B.; Staquicini, F. I.; Soghomonyan, S.; Alauddin, M. M.; Benjamin, R. S.; Pollock, R. E.; Gelovani, J. G.; Pasqualini, R.; Arap, W. *Proc. Natl. Acad. Sci. U.S.A.* **2008**, *105*, 4471.

(169) Hajitou, A.; Trepel, M.; Lilley, C. E.; Soghomonyan, S.; Alauddin, M. M.; Marini, F. C.; Restel, B. H.; Ozawa, M. G.; Moya, C. A.; Rangel, R.; Sun, Y.; Zaoui, K.; Schmidt, M.; von Kalle, C.; Weitzman, M. D.; Gelovani, J. G.; Pasqualini, R.; Arap, W. *Cell* **2006**, *125*, 385.

(170) Houimel, M.; Schneider, P.; Terskikh, A.; Mach, J. P. *Int. J. Cancer* **2001**, *92*, 748.

(171) Urbanelli, L.; Ronchini, C.; Fontana, L.; Menard, S.; Orlandi, R.; Monaci, P. *J. Mol. Biol.* **2001**, *313*, 965.

(172) Stortelers, C.; Souriau, C.; van Liempt, E.; van de Poll, M. L.; van Zoelen, E. J. *Biochemistry* **2002**, *41*, 8732.

(173) Arap, M. A.; Lahdenranta, J.; Mintz, P. J.; Hajitou, A.; Sarkis, A. S.; Arap, W.; Pasqualini, R. *Cancer Cell* **2004**, *6*, 275.

(174) Chen, L.; Hnatowich, D.; Rusckowski, M. *J. Nucl. Med. Meet. Abstr.* **2007**, *48*, 310P.

(175) Rusckowski, M.; Gupta, S.; Liu, G.; Dou, S.; Hnatowich, D. J. *Cancer Biother. Radiopharm.* **2007**, *22*, 564.

(176) Nothelfer, E. M.; Zitzmann-Kolbe, S.; Garcia-Boy, R.; Kramer, S.; Altmann, A.; Eisenhut, M.; Mier, W.; Haberkorn, U. *J. Nucl. Med.* **2009**, *50*, 426.

(177) Laakkonen, P.; Akerman, M. E.; Biliran, H.; Yang, M.; Ferrer, F.; Karpanen, T.; Hoffman, R. M.; Ruoslahti, E. *Proc. Natl. Acad. Sci. U.S.A.* **2004**, *101*, 9381.

(178) Kridel, S. J.; Chen, E.; Howard, E. W.; Mobashery, S.; Smith, J. W. *J. Biol. Chem.* **2001**, *276*, 20572.

(179) Pan, W.; Arnone, M.; Kendall, M.; Grafstrom, R. H.; Seitz, S. P.; Wasserman, Z. R.; Albright, C. F. *J. Biol. Chem.* **2003**, *278*, 27820.

(180) Ke, S. H.; Coombs, G. S.; Tachias, K.; Corey, D. R.; Madison, E. L. *J. Biol. Chem.* **1997**, *272*, 20456.

(181) Yang, S. Q.; Craik, C. S. *J. Mol. Biol.* **1998**, *279*, 1001.

(182) Fong, S.; Goodson, R. J.; Drummond, R. J.; Stratton, J. R.; McGuire, L.; Doyle, L. V.; Chapman, H. A.; Rosenberg, S. *Biol. Chem.* **2002**, *383*, 149.

(183) Shao, R.; Xiong, C.; Wen, X.; Gelovani, J. G.; Li, C. *Mol. Imaging* **2007**, *6*, 417.

(184) Martens, C. L.; Cwirla, S. E.; Lee, R. Y.; Whitehorn, E.; Chen, E. Y.; Bakker, A.; Martin, E. L.; Wagstrom, C.; Gopalan, P.; Smith, C. W.; et al. *J. Biol. Chem.* **1995**, *270*, 21129.

(185) Kelly, K.; Alencar, H.; Funovics, M.; Mahmood, U.; Weissleder, R. *Cancer Res.* **2004**, *64*, 6247.

(186) Spear, M. A.; Breakefield, X. O.; Beltzer, J.; Schuback, D.; Weissleder, R.; Pardo, F. S.; Ladner, R. *Cancer Gene Ther.* **2001**, *8*, 506.

(187) Mintz, P. J.; Cardo-Vila, M.; Ozawa, M. G.; Hajitou, A.; Rangel, R.; Guzman-Rojas, L.; Christianson, D. R.; Arap, M. A.; Giordano, R. J.; Souza, G. R.; Easley, J.; Salameh, A.; Oliviero, S.; Brentani, R. R.; Koivunen, E.; Arap, W.; Pasqualini, R. *Proc. Natl. Acad. Sci. U.S.A.* **2009**, *106*, 2182.

(188) Bockmann, M.; Drosten, M.; Putzer, B. *J. Gene Med.* **2005**, *7*, 179.

(189) Kennel, S. J.; Mirzadeh, S.; Hurst, G. B.; Foote, L. J.; Lankford, T. K.; Glowienka, K. A.; Chappell, L. L.; Kelso, J. R.; Davern, S. M.; Safavy, A.; Brechbiel, M. W. *Nucl. Med. Biol.* **2000**, *27*, 815.